# annual report 1986

nuclear physics laboratory
university of washington

ANNUAL REPORT


Nuclear Physics Laboratory
University of Washington
April, 1986

## INTRODUCTION

This is our annual report for the year ending in April, 1986. It summarizes the work done in the Nuclear Physics Laboratory and the experiments we have carried out at other laboratories.

Visitors to our Laboratory have commented on the noticeable transformations which have been taking place this year as a result of the booster accelerator project. Major pieces of the booster are moving to their permanent positions on the floor. Once again, the size of the laboratory staff has increased and there is a growing sense of accomplishment and anticipation. Over one third of the final accelerator, plus the beam transport system from the tandem to the booster, are already in place (June 1, 1986) and we are looking forward to tests, with beam, of this first part of the machine. At the same time the installation of the rest of the accelerator will continue and is expected to be completed on the original schedule, by the end of 1986.

Other technical developments include the recent move of the polarized ion source to its permanent location. Just before this move, the source produced 700 nA of polarized beam through the spin processor. The cesium beam component of the new source has already been tested at the final site and was found to give the very good performance it had given earlier.

Technical improvements have continued on the tandem itself. The sputter ion source for example has had its stability improved and its negative ion output substantially increased. A stand-alone helium ion source has been put together from part of the old Lamb Shift polarized ion source and has already provided beam.

The spectrum of research interests pursued by the laboratory staff continues to be broad. One of the more interesting heavy ion studies involves the determination of the spin-distributions of the compound nuclei which are formed in sub-barrier fusion. Fission fragment anisotropies were used to determine the mean square spin values of such compound nuclei. In $^{12}C + ^{238}U$ and in $^{16}O + ^{232}Th$ these values were found to be more than twice as large as expected. To understand the possible role of collectivity in this anomaly we have also studied $^{16}O + ^{208}Pb$ (where the target is spherical). Here the anomaly is smaller, even disappearing at the lowest bombarding energies. For this reaction the experimental results can be compared with an usually complete coupled-channels calculation that includes both inelastic and transfer channels.

Total reaction cross sections for nucleus-nucleus scattering have been measured with $^{12}C$ beams at $E/A = 10-35$ MeV/AMU. This work shows surprisingly good agreement with simple Glauber model predictions. The elastic scattering measurements from which the total reaction cross sections were obtained also show evidence for the failure of the M3Y double folding model at 36 MeV/AMU.

1

In the area of symmetry studies, considerable progress has been made in the Washington-Wisconsin experiment to measure parity-mixing in $^{19}N$. With the aid of a strip-target beam-scanner it was possible to show that the main sources of systematic error are residual transverse polarization gradients in a nominally longitudinally polarized beam. The origins of these gradients in the University of Wisconsin ion source are being tracked down.

A new iron-free solenoid system for the parity non-conservation experiment on hydrogen has been temporarily installed on temporary supports in the experimental area. The field non-uniformities and hysteresis effects are now less than 5 parts in $10^3$, a factor of 50 times better than the old solenoid system.

In collaboration with the atomic physics group in this department an experiment to accurately compare the masses of proton and antiproton has begun. The latter will be measured at CERN to $\sim 1$ part in $10^8$ and the former will be measured here in Seattle. The comparison would improve the test for CPT invariance for baryons by a factor of $10^5$. A first run at CERN has demonstrated the feasibility of slowing down a significant number of protons to 1 keV, an energy at which they can be captured in a Penning trap.

Our extensive survey of the statistical decay of the giant dipole resonance (GDR) built upon excited states has continued. These studies cover a wide mass range and provide new information on the decay of the GDR at temperatures from 1 to 2 MeV and spins between 10 and 25ħ. The mean resonance energy is found to vary smoothly with mass and to agree with photoabsorption studies on ground states. The total resonance strengths are found to correspond to one classical sum-rule. In $^{60}Co$, for example, the resonance energy and strength do not change over a wide range of excitation and spin while the width increases considerably as the excitation and spin increase, presumably reflecting the changes in the distribution of compound nuclear deformations.

An analysis of the fore-aft asymmetry in the $(\gamma,n)$ reaction in $^{208}Pb$, performed in collaboration with the University of Illinois, shows that the location ($\sim 23$ MeV) of the E2 isovector resonance can be deduced from these data with relatively little ambiguity. The width of this resonance is larger than that of the E1 isovector resonance, but its value cannot be determined with precision because of uncertainties in the phases of the odd and even parity amplitudes whose interference is responsible for the asymmetry.

The quasi-elastic scattering of $\pi^+$ and $\pi^-$ on $^2H$, $^3He$ and $^4He$ is being studied with several models to compare with the precise experimental results for the relative cross-sections at 100 MeV which we obtained at TRIUMF. A particular problem is that of understanding the role of the pion absorption in accounting for the small ratio ($\sim 0.6$) of the $^4He/^3He$ cross-sections.

In the accelerator mass spectrometry (AMS) program, two new collaborative efforts have been undertaken with colleagues in the Oceanography Department, one on organic $^{14}C$ concentrations in the surface layers of the deep-sea sediments and one on methane cycling in Alaskan tundra, a high-

northern-latitude wetland environment significant in the global methane picture. (The latter study is supported primarily by NASA.)

We close this introduction with a reminder that the articles in this report describe work in progress and are not to be regarded as publications or quoted without permission of the investigators. In each article the names of the investigators have been listed alphabetically, but where appropriate the names of those primarily responsible for the report have been underlined.

As always, we welcome applications from outsiders for the use of our facilities. As a convenient reference for potential users, the table on the following page lists the vital statistics of our accelerators. For further information please write or telephone Dr. W.G. Weitkamp, Technical Director, Nuclear Physics Laboratory, University of Washington, Seattle, WA 98195; (206) 543-4080.

We are grateful to Barbara Fulton for her contributions to the design and production of this report.

<div align="center">

I. Halpern

Editor

</div>

## TANDEM VAN DE GRAAFF ACCELERATOR

A High Voltage Engineering Corp. Model FN purchased in 1966 with NSF funds; operation funded primarily by the U.S. Department of Energy. See W.G. Weitkamp and F.H. Schmidt, "The University of Washington Three Stage Van de Graaff Accelerator," Nucl. Instrum. Meth. 122, 65 (1974).

### Available Energy Analyzed Beams:

| Ion | Max. Current (pμA) | Max. Practical Energy (MeV) |
|-----|-----|-----|
| p,d | 20 | 18 |
| He | 1.5 | 27 |
| Li | 0.2 | 36 |
| C | 1.8 | 63 |
| N | 0.2 | 62 |
| O | 1 | 72 |
| Si | 0.1 | 90 |
| Cl | 0.2 | 90 |
| Ni | 0.005 | 99 |
| Br | 0.05 | 108 |
| Ag | 0.001 | 108 |

## 60-INCH CYCLOTRON

A fixed energy cyclotron constructed in 1950-52 with State of Washington funds; operated with income from outside users. See F.H. Schmidt, G.W. Farwell, J.E. Henderson, T.J. Morgan, and J.F. Streib, "The University of Washington Sixty-Inch Cyclotron," Rev. Sci. Instrum. 25, 499 (1954).

### Available Target Box Beams:

| Ion | Maximum Current (μA) | Energy (MeV) |
|-----|-----|-----|
| p | 100 | 11 |
| d | 150 | 22 |
| ⁴He | 30 | 42 |

# TABLE OF CONTENTS

## 15.   APPENDIX

1.  ASTROPHYSICS AND COSMOLOGY

## 1.1  Search for a γ-Branch of the Unbound 5.17 MeV Level of $^{14}O$

E.G. Adelberger, P.B. Fernandes, and M.A. Khandaker

In massive stars of the main sequence (where T≈20×10⁶ K), the main mechanism for energy production is believed to be the burning of hydrogen in the CNO cycle:

$$^{12}C(p,\gamma)^{13}N(\beta^+)^{13}C(p,\gamma)^{14}N(p,\gamma)^{15}O(\beta^+)^{15}N(p,\alpha)^{12}C$$

As the temperature increases, $^{13}N(p,\gamma)$ opens up as an alternative channel for destruction of $^{13}N$, triggering the so-called "hot" CNO cycle:

$$^{12}C(p,\gamma)^{13}N(p,\gamma)^{14}O(\beta^+)^{14}N(p,\gamma)^{15}O(\beta^+)^{15}N(p,\alpha)^{12}C$$

At proton energies that occur in stars (≈few keV), the $^{13}N(p,\gamma)$ cross-section is dominated by the L=0, 547 keV resonance in $^{14}N$+p, and we can write

$$\sigma(E) = \frac{\pi\hbar^2}{2mE} \frac{2J_R+1}{[2J_i+1][2J_p+1]} \frac{\Gamma_\gamma\Gamma_p}{[E-E_R]^2+\frac{\Gamma^2}{4}}$$

where $\Gamma=\Gamma_\gamma+\Gamma_p$ is the total width of the 5.17 MeV, 1⁻ level in $^{14}O$. The measured value of $\Gamma$ is 38.1±1.8 keV,[1] while theoretical calculations yield $\Gamma_\gamma=1.5-5$eV,[2] or a predicted γ-branch $\Gamma_\gamma/\Gamma≈10^{-4}$.

We use the reaction $^{12}C(^3He,n)$ at a beam energy of 9.4 MeV, and search for γ rays in coincidence with neutrons populating the 5.17 MeV level in $^{14}O$. Our apparatus consists of two gain-stabilized 5"×6" NaI detectors located at 90° one on each side of the target and 3 cm apart, and a liquid scintillator detector at 0° (the neutron flight path is 60 cm). The liquid scintillator coupled to a pulse shape discriminator module yields excellent n-γ discrimination. Lead shielding around the γ detectors reduces γ-γ and random coincidences.

The target is 100 μg/cm² of isotopically enriched $^{12}C$ (99.985%) evaporated onto a 20 mil Au (99.9985%) backing. To keep the carbon build-up to a minimum, we have a cold trap just upstream from the target. We searched for contaminants by bombarding our target with 4 MeV protons and observing the γ-ray spectrum with a Ge(Li) detector. We identified and measured amounts of Al, N and NaCl.

Preliminary runs yield $\Gamma_\gamma/\Gamma≈(-1.2±2.8)×10^{-4}$ (assuming an isotropic n-γ angular correlation). Unknown contaminants on our target are the limiting factor at the moment. Our next step will be to obtain a "cleaner" target (we are considering making a gas target of enriched $CH_4$).

References:

1.  T.E. Chupp, R.T. Kouzes, A.B. McDonald, P.D. Parker, T.F. Wang, and A. Howard, Phys. Rev. C 31, 1023 (1985).
2.  K. Langanke, O.S. van Roosmalen, and W.A. Fowler, Nucl. Phys. A 435, 657 (1985).

## 1.2 Energy Shifts for Gamma Rays From Interactions in Interstellar Grains

D. Bodansky and D.D. Leach

Gamma-ray lines from nuclear reactions in grains, e.g., interstellar grains, will be narrow if the decay lifetimes are more than about 1 psec.[1] This fact has been used by Ramaty, Kozlovsky, and Lingenfelter (RKL)[1] to explain the reported narrow line at 1497 keV from SS433[2] as well as a possible but uncertain line from SS433 at 6695 keV. In the RKL model, these lines (if confirmed) are the Doppler-shifted 1369-keV $^{24}$Mg and 6129-keV $^{16}$O lines, with mean lives of 1.98 psec and 27 psec.

We consider the further shift in the mean $\gamma$-ray energy which occurs when an appreciable fraction of the $\gamma$ rays are emitted before the recoil nuclei stop in the grain. Unless the decay time is very much greater than the stopping time, the observed line will be shifted from the fully stopped position. This slowing down shift, $\Delta E$, defined here as the difference between the mean energy of the observed peak and the energy for emission from a nucleus at rest, can be determined from laboratory measurements.[4] For the $^{24}$Mg(p,p')$^{24}$Mg reaction at $E_p$ =22 MeV, the shift extrapolated to 0° is found to be $\Delta E$=2.9 keV. (The calculated shift for $^{24}$Mg moving initially at the center-of-mass velocity is $\Delta E$≈2.76 keV.)

In the RKL model for SS433, the 1369-keV line is Doppler shifted to 1497 keV due to the motion, at a speed corresponding to 33 MeV per nucleon, of magnesium-rich grains through hydrogen. The slowing down shift comes from the recoil of the $^{24}$Mg backwards with respect to the motion of the grain. Ignoring the slowing down effects, the Doppler shift is the same for all lines. A 6129.2-keV $\gamma$ ray would be observed at 6704 keV (if a 1368.6-keV $\gamma$ ray is observed at 1497 keV. The magnitude of the slowing down shift for $^{24}$Mg has been calculated from the experimental value of $\Delta E$ at $E_p$=22 MeV, using a crude extrapolation where $\Delta E$ varies as $E^{0.5}$. The shift is smaller for the 6129-keV line and an approximate calculation was made. The overall effect of the two shifts is to raise the predicted energy of a 6129-keV line from 6704 keV to 6707 keV.

Whether a shift of this magnitude is significant for SS433, or in other similar cases, depends on the nature of the observational data. Precise knowledge of the expected peak position is particularly useful in cases where enough counts are seen to give an indication of a line but where the $\gamma$-ray flux is too small to see more than one line from a given nuclide. SS433 may turn out to be such an instance, although here the observation even of the line at 1497 keV awaits confirmation.

References:

1. R.E. Lingenfelter and R. Ramaty, Astrophys. J. 211, L19 (1977).
2. R. Ramaty et al., Astrophys. J. 283, L13 (1984).
3. R.C. Lamb et al., Nature 305, 37 (1983).
4. P. Dyer et al., Phys. Rev. C 23, 1865 (1981).

2

## 1.3 Nucleosynthesis of $^{180}Ta^m$

### S.E. Kellogg and E.B. Norman[*]

The source of the naturally-occurring isomer $^{180}Ta^m$ remains an astrophysical puzzle. Our efforts in the last few years have concentrated on measuring weak $\beta$-decay rates which can yield $^{180}Ta^m$ in the standard slow (s) and/or rapid (r) neutron capture processes. Such a production mechanism was first proposed by Beer and Ward[2]. We have established a restrictive limit on the 214 keV endpoint $\beta$-decay branch $f_\beta$ from the 5.5 hour isomer $^{180}Hf^m$ directly to $^{180}Ta^m$ of 0.35% which is good enough to exclude a dominant s-process contribution to the $^{180}Ta$ abundance. This limit corresponds to a lower bound on the log-ft value for the $I^\pi, K = (8^-, 8)$ to $(9^-, 9)$ allowed, hindered Gamow-Teller transition of 6.4, which compares with the value of 6.4 measured in the analogous decay of $^{180}Hf^m$[1]. Further, the s-process contribution to the abundance of $^{180}Ta$ is limited to less than 35%.

Our attention has shifted therefore to the r-process contribution which requires that a fraction $f_r$ of the $I^\pi, K = (3^-, 3)$ $^{180}Lu$ 5.5 minute $\beta$-decay yield feeds $^{180}Hf^m$. Our limit of $f_r \leq 0.06\%$ obtained by radiochemical separation of Lu from Hf following the $^{180}Hf(n,p)$ reaction[2] is in disagreement with Eschner et al.'s reported value of $f_r = 0.46 \pm 0.15\%$[3]. Such a discrepancy in experimental results might be explained if there exists a high-spin, short-lived isomer of $^{180}Lu$. Likely $J^\pi$ candidates are $8^-$ and $9^-$ (structurally identical to the low-lying high-spin states in $^{180}Ta$) and recent calculations indicate that these two levels should lie within 200 keV of the $3^-$ ground state.[4] A series of "rabbit" experiments at the Berkeley 88" Cyclotron were attempted to produce a $^{180}Lu$ isomer with a 10 sec to 1 minute halflife to be detected by looking for the ingrowth in the strong ground-state $\gamma$-decay lines. No evidence for the production in the (n,p) reaction of an isomer with a halflife greater than 20 seconds was seen partly due to the strong 7 sec halflife decay of $^{24}N$ produced in the oxide target. The motivation for the continuation of such a search lies in the dearth of any experimental limits on the stellar conditions which prevail during and immediately after the r-process, whose very site remains unestablished. A low-energy, high-spin isomer in $^{180}Lu$ equilibrated with ground-state, might hand down this high spin through the isomer in $^{180}Hf$ to $^{180}Ta$. Under very specific conditions, the $^{180}Ta^m$ produced depends on the time-temperature dynamics of the post-r-process.

### References:

* Lawrence Berkeley Laboratory, University of California, Berkeley, CA 94720.
1. H. Beer and R. Ward, Nature 291, 308 (1981).
2. Nuclear Physics Laboratory Annual Report, University of Washington (1983) p. 1; ibid. (1984) p. 3; ibid. (1985) p. 1.
3. W. Eschner et al., Z. Phys. A317, 281 (1984).
4. R. Hoff, private communication.

2.    GIANT RESONANCES IN EXCITED NUCLEI

## 2.1   Systematic Behavior of the Statistical Decay of the Giant Dipole Resonance in Highly Excited Nuclei

J.A. Behr, G. Feldman, C.A. Gossett, J.H. Gundlach, M. Kicinska-Habior, and K.A. Snover.

Over the past two years the statistical decay of the giant dipole resonance from highly excited nuclei has been studied extensively in our laboratory for nuclei from A ~ 40 to 170 (See Ref. 1 and Secs. 2.4, 2.5, 2.6, 2.8). A summary of these studies is presented in the figure below. The solid curves in the figure represent the approximate behavior of the ground state GDR. Roughly one unit of the classical dipole sum rule strength is exhausted in each case for the decay of highly excited nuclei. The mean resonance energy is found to vary smoothly with mass number and with the exception of $^{44}$Ti and $^{63}$Cu, is in good agreement with the resonance energy for the ground state GDR. In general only the T component of the isospin split GDR is excited in complex particle collisions, and the magnitudes of the discrepancies in the resonance energy in the mass 46 and 63 cases are understood in terms of isospin splitting, which has the largest effect in light nuclei. The width of the GDR in highly excited nuclei is perhaps the most interesting feature. In regions of strong deformation, A ~ 70-80 and A ~ 150-170, for which the width of the GDR built on the ground state is dominated by deformation splitting, we find that in detail the shape of the GDR built on excited states is the same as that observed for the ground state.[2] In nuclei which do not have large static deformation we find excited-state GDR widths which are considerably broader[2] than expected from ground state photoabsorption. We believe this results from the effect that at finite temperature the ensemble of excited nuclear states populated by the γ decay has a distribution of deformation.[3] Our results are consistent with the concept of a limiting temperature,[3] T ~ 40δA$^{1/3}$ MeV, up to which nuclei should retain the deformation of the ground state. In a strongly deformed nucleus in the rare earth region for example, A=160, δ=0.3, the limiting temperature is ~ 2.2 MeV, while for A=120, δ=0.1, T ~ 0.8 MeV. Hence in our studies of Er nuclei in which the mean final state temperatures are approximately 1 MeV, one expects the shape of the GDR at high excitation to be similar to the shape of the ground state GDR, while for studies in the tin region for which the mean final state temperatures are about 1.5 MeV, one expects the γ decays to be averaging over an ensemble of nuclear states with a distribution of deformation.

References:

1.  Nuclear Physics Laboratory Annual Report, University of Washington (1985) pp. 9, 11, 14, 20.

2.  C.A. Gossett, K.A. Snover, J.A. Behr, G. Feldman and J.L. Osborne, Phys. Rev. Lett. 54, 1486 (1985), Nuclear Physics Laboratory Annual Report, University of Washington (1985) pp. 9, 14; and Sec. 2.6 of this report.

3.  S. Bjornholm et al., in Proceedings of the Third Symposium on the Physics and Chemistry of Fission, Rochester, 1973 (IAEA, Vienna, 1974), Vol. 1, p. 367.
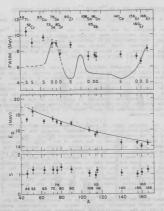
Fig. 2.1 Properties of the statistical decay of the GDR in highly excited nuclei as a function of mass number. Top: Full width at half maximum of the GDR strength function. Middle: Mean dipole resonance energy. Bottom: Fraction of classical dipole sum rule strength exhausted in statistical GDR decay. The fitted strengths (calculated without regard to isospin) were corrected by factors of 1.6-1.1 for A=46-166 to account for the fact that the experiments are sensitive to only the T< component of the GDR. Curves represent approximate behavior of the ground state GDR. Data for decays of highly excited nuclei are labeled by the initial compound nucleus as well as by S or D for analyses in which either a single or double component Lorentzian form was used for the GDR strength function.

5

## 2.2 Excited-State GDR's in $^{48}$Ti and $^{52}$Cr via the (p,$\gamma$) Reaction

J.A. Behr, G. Feldman, C.A. Gossett, J.H. Gundlach, and K.A. Snover

The analysis of our data from the $^{47}$Sc(p,$\gamma$)$^{48}$Ti and $^{51}$V(p,$\gamma$)$^{52}$Cr radiative capture reactions over the energy range $E_x \approx 4.0$-23.5 MeV is nearing completion. Our intention is to understand the relation between GDR capture strength to excited final states and single-particle strength at these excitation energies. The details of the experiment and analysis procedure were described in last year's Annual Report.[1]

We have now obtained absolute ($\gamma$,p$_0$) cross sections (converted from (p,$\gamma$) by detailed balance) as a function of $\gamma$-ray energy. All the excitation curves show broad resonance bumps in the vicinity of $E_x = 18$ MeV. Estimates of the statistical contribution to the observed cross sections have been calculated using the compound nuclear evaporation code CASCADE[2] (see Sec. 2.4). The difference between the measured ($\gamma$,p$_0$) GDR cross section and the calculated statistical component is assumed to be the direct plus semi-direct GDR strength, which is expected to correlate with the proton-stripping spectroscopic factors for the final states in the residual nucleus populated in the (p,$\gamma$) reaction.

In the extreme limit of equal penetrabilities for all nucleon decay channels, a proportionality can be derived[3] between the integrated ($\gamma$,p$_0$) strengths and the proton-stripping spectroscopic factors. The success of this model was demonstrated earlier in the case of the $^{27}$Al(p,$\gamma$)$^{28}$Si reaction.[4] In the present study of $E_{X,2}$ ground-state transitions, however, the extreme approximation is inadequate, as it predicts too much $\ell$=3 strength relative to the data. In the comparison of our integrated ($\gamma$,p$_0$) data to $C^2S$[5,6] (shown in Fig. 2.2), an attempt has been made to account for barrier penetration effects in a crude manner by scaling down the spectroscopic factors[5,6] for $\ell$=3 proton transfers by the ratio $P_1(E)/P_3(E)$ of $\ell$=1 and $\ell$=3 penetrabilities. In spite of the simplicity of this penetrability approximation, the results show a reasonable correlation between the integrated GDR strength and the spectroscopic strength.

A more detailed calculation based on the schematic model of the GDR (see Sec. 2.10), which implicitly includes energy- and $\ell$-dependent penetrability factors $P_\ell(E)$ in the competition of the various nucleon decay channels, is currently in progress.

### References:

1. Nuclear Physics Laboratory Annual Report, University of Washington (1985) p. 18.
2. F. Pühlhofer, Nucl. Phys. A $\underline{280}$, 267 (1977).
3. K.A. Snover, Journal de Physique $\underline{45}$, C4-337 (1984).
4. D.H. Dowell, G. Feldman, K.A. Snover, A.M. Sandorfi and M.T. Collins, Phys. Rev. Lett. $\underline{50}$, 1191 (1983).
5. J.R. Beene, Nucl. Data Sheets $\underline{25}$, 235 (1978).
6. R.L. Auble, Nucl. Data Sheets $\underline{24}$, 1 (1978).
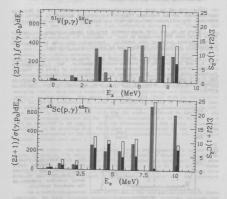
Fig. 2.2 Comparison of integrated GDR capture strength to excited final states in the reactions $^{51}V(p,\gamma)^{52}Cr$ and $^{45}Sc(p,\gamma)^{46}Ti$ (left-hand bars) vs. spectroscopic strength[9] (right-hand bars). The right-hand bars are coded so as to indicate the relative contributions of $\ell=1$ (open bars) and $\ell=3$ (solid bars) spectroscopic factors. In addition, the $\ell=3$ values of $C^2S$ have been multiplied by a penetrability factor $P_1(E)/P_3(E)$ (see text). The scales on the left-hand and right-hand axes are related by a proportionality factor of 30 MeV-mb.

1. D. Reichmack Nucl. Phys. A 290, 459 (1977).

2. S.E. Kennett et al., Phys. Lett. 105B 15 (1981).

## 2.3 NaI Detector Efficiencies and $^{11}B(p,\gamma)$ Cross Section

J.A. Behr, G. Feldman, H.K. Glatzel, C.A. Gossett, J.H. Gundlach,
M. Kicinska-Habior, and K.A. Snover

Our goal is to work toward a precision measurement of the absolute cross-section of the reaction $^{11}B(p,\gamma)$ for energies between 20 and 30 MeV. Therefore the efficiency of our 10"×10" NaI detector needs to be determined.

Since we do not have experimental data for these energies, we use the Monte Carlo code EGS developed at SLAC[1] to simulate the electron-$\gamma$-ray-showers in the various parts of the detector. Previously the code has been successfully used to calculate efficiencies of scintillation detectors.[2]

To check our simulation we analyzed data taken by P. Fernandez[3] at 2.3, 4.9, 8.3 and 15.1 MeV for the neutron-shielded detector. Ref. 3 describes the measured efficiency data. Efficiencies with an accuracy of 3%-4% and response functions were obtained. The measured and calculated total response functions for $E_\gamma$=4.9 MeV are shown in Fig. 2.3. The data are from p-$\gamma$ coincidence measurements of the decay of $^{13}N$ (4.9 MeV) produced by the $^{12}C(^3He,p)$ reaction.
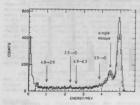


Fig. 2.3 Calculated (histogram) and measured lineshape at 4.9 MeV. Arrows mark the position of weak decay branches present in the measured spectrum.

## References:

1. SLAC-reports: SLAC-210 and SLAC-265.
2. D.W.O. Rogers, Nucl. Instrum. Methods A 199, 531 (1982).
3. Nuclear Physics Laboratory Annual Report, University of Washington (1985) p. 65.

## 2.4 Statistical Decay of the Giant Dipole Resonance in $^{46}$Ti and $^{52}$Cr

J.A. Behr, G. Feldman, C.A. Gossett, J.H. Gundlach, and K.A. Snover

As a means of understanding the statistical decay of the GDR in $^{46}$Ti and $^{52}$Cr (which is relevant for the (p,y) studies discussed in Sec. 2.2), we have measured inclusive γ-ray spectra from the heavy-ion fusion reactions $^{19}$F+$^{27}$Al→$^{46}$Ti and α+$^{48}$Ti→$^{52}$Cr at four bombarding energies (E($^{19}$F)=30-60 MeV) corresponding to excitation energies in $^{46}$Ti of 39.5-58.1 MeV and $E_\alpha$=12-28 MeV corresponding to excitation energies in $^{52}$Cr of 20.4-35.2 MeV). Preliminary results appeared in last year's Annual Report.[1] These reactions also provide valuable information relevant to the study of the systematics of the GDR in highly-excited nuclei over a wide range of energy and spin throughout the periodic table.

After correcting the data for pileup and neutron-induced events, we have extracted GDR parameters by fitting the γ-ray spectra with a statistical model calculation using the compound nuclear evaporation code CASCADE.[2] The GDR energies remain relatively constant with bombarding energy but differ from one reaction to the other. The lower GDR energy value (E=17 MeV) in the case of $^{19}$F+$^{27}$Al can be understood in terms of isospin splitting by recognizing that the heavy-ion fusion channel will only populate the T$_<$ component of the GDR. This result is also consistent with the GDR energy obtained by Sandorfi[3] for the same compound nucleus in the $^{16}$O+$^{28}$Si reaction. The α+$^{48}$Ti result (E=18 MeV) is expected to be similar, and the discrepancy in GDR energy is somewhat puzzling. It is possible that the higher resonance energy in the latter case may be a consequence of the onset of non-statistical effects in the α-particle entrance channel (see Sec. 2.9).

In all cases, the widths are large (Γ≈8-12 MeV) compared to ground-state values (typically Γ<6 MeV). In the $^{19}$F+$^{27}$Al case, a monotonic increase in width is apparent with increasing excitation energy and spin. All cases show a GDR strength near or slightly in excess of a full E1 sum rule. These strengths have been adjusted to take isospin and parity effects properly into account and therefore reflect a reasonable estimate for the strength parameter.

As a model-independent means of checking the statistical nature of these reactions, we have obtained angular distributions at selected energies and have fitted the results with a Legendre polynomial expansion. The data indicate a nearly isotropic angular dependence, consistent with the assumption of a statistical decay mechanism. In light of this result, any firm conclusions about the α+$^{48}$Ti case will have to await further study.

References:

1. Nuclear Physics Laboratory Annual Report, University of Washington (1985), p. 20.

2. F. Puhlhofer, Nucl. Phys. A 280, 267 (1977).

3. A.M. Sandorfi et al., Phys. Lett. 130B, 19 (1983).

## 2.5 Statistical GDR Decay of Highly Excited States of $^{63}Cu$

J.A. Behr,  G. Feldman,  H. Glätzel,  C.A. Gossett,  J.H. Gundlach,
M. Kicinska-Habior, and K.A. Snover

Very little information is available on the dependence of statistical GDR decay as a function of temperature and spin in a given nucleus.[1,2] The purpose of the present work is to examine the GDR decay of the equilibrated hot nucleus $^{63}Cu$ and search for a possible dependence of the GDR energy, width and strength on the nuclear temperature and spin.
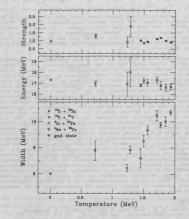
In order to populate states of $^{63}Cu$ at the same excitation energy, but with different initial spin distributions, we have examined different reaction entrance channels with $^{16}O$, $^{12}C$, $^{7}Li$ and $^{4}He$ as a projectile. We have measured continuum γ-ray spectra from decays of $^{63}Cu$ formed at initial excitation energies of 22.5 and 32.4 MeV, 32.0, 39.5 and 52.0 MeV, 34.7, 39.5, 52.2 and 65.7 MeV, 52.2, 61.6 and 77.4 MeV in $^{47}He+^{59}Co$, $^{7}Li+^{56}Fe$, $^{12}C+^{51}V$, and $^{16}O+^{47}Sc$ reactions, respectively. The average initial spin of the populated states varies from 2 to 23 ℏ. The experimental γ-ray spectra from different reactions with the same initial excitation energy have very similar shapes, in agreement with the hypothesis that compound nuclear decays should be independent of the entrance channel.

Non-linear least squares fitting of the statistical model calculation to the data was performed to extract parameters of the GDR strength function (energy $E_D$, width Γ and E1 sum rule strength fraction S). Except for the cases of $^{4}He$ and $^{7}Li$ at the highest bombarding energies (see below) we have found that the GDR parameters for the same excitation energy but different entrance channels are the same within experimental error, indicating at most a weak spin dependence. The mean energy $E_m$=16.9±0.3 MeV and strength S=0.98±0.17 of the GDR at finite temperature are close to the ground state values, while the width varies smoothly from 6.5±0.3 MeV to 10.7±0.2 MeV in the temperature range from 0.7 MeV to 1.9 MeV, as shown in Fig. 2.5. These results are consistent with theoretical expectations that the GDR strength and energy should not change as a function of temperature and spin, while the width should broaden at higher temperature due to thermal averaging over a distribution of deformations.[3]

Both $^{4}He$- and $^{7}Li$-induced reactions show evidence for nonstatistical effects at the highest bombarding energies. In order to further check the character of $^{7}Li$ induced reactions we have also measured $^{7}Li+^{159}Tb \rightarrow ^{166}Ho \rightarrow ^{165}Ho$ and $^{4}Li+^{161}Ta \rightarrow ^{170}Os$ to compare with $^{6}Li+^{57}Fe \rightarrow ^{63}Cu$ at the same bombarding energy of $E(^{7}Li)$=36.8 MeV. We have found that the nonstatistical yield of γ rays in the giant resonance for the $^{7}Li$ channel increases with the target mass and is significant for $^{165}Ta$ as a target, while for $^{57}Fe$ the γ spectra can be still reproduced by statistical model calculations with reasonable GDR parameters.

References:

1. Nuclear Physics Laboratory Annual Report, University of Washington (1985) p. 20

2. J.J. Gaardhoje et al., Phys. Rev. Lett. **56**, 1783 (1986).

3. M. Gallardo et al., Nucl. Phys. A **443**, 415 (1985).

Fig. 2.5 Parameters of the GDR strength function of $^{63}$Cu for different values of nuclear temperature.

## 2.6 Giant Dipole Resonances in Highly Excited Nuclei in the Mass Region A≈70-90

J.A. Behr, G. Feldman, J.H. Gundlach, C.A. Gossett, and K.A. Snover

We used the following heavy ion fusion reactions: $^{12}C + ^{60,61,64}Ni \rightarrow ^{72,73,76}Se$, $^{16}O + ^{61,64}Ni \rightarrow ^{77,80}Kr$, $^{16}O + ^{64}Zn \rightarrow ^{80}Sr$, and $^{16}O + ^{72}Ge \rightarrow ^{88}Zr$ to produce highly excited compound nuclei ($E_x \approx 40$-50 MeV). In the cooling down process these nuclei emit mainly particles but also energetic $\gamma$-rays. The $\gamma$-ray spectra were measured with the 10"×10" anticoincidence and lead shielded NaI(Tl) detector. By using the time of flight technique involving a pulsed beam, prompt $\gamma$-ray events could be separated from fast neutrons. This together with wax shielding and pileup rejection resulted in a clean statistical $\gamma$-ray spectrum up to very high energies ($E_\gamma \approx 25$ MeV).

All cases clearly display the bump in the exponential $\gamma$-ray spectrum which is due to GDR decays from the hot compound nucleus. The statistical model code CASCADE, was fitted to the data and up to six parameters in the assumed E1 strength function were varied simultaneously, resulting in a good fit over six decades in $\gamma$-ray yield. In the cases of $^{72,76}Se$ and $^{80}Sr$ a two Lorentzian component strength function was necessary to describe the data, while one component was sufficient for the $^{80}Zr$ data. A comparison with available data from $(\gamma,n)$-reactions[1] ($^{76}Se$,$^{90}Zr$) which probe the GDR built on the ground state shows that the resonance energy is almost the same for the excited state GDR as for the ground state GDR. Furthermore the integrated strength turns out to be very close to one classical E1 sum rule as is observed in $\gamma$-absorption measurements on the ground state. In the hydrodynamical model[2] the energy separation and strength distribution of the two GDR components is closely related to the nuclear shape. The deduced strength ratios $S_1/S_2$ indicate that the (assumed axially symmetric) excited nuclei are prolate, in agreement with low energy data[3], while the deformation magnitude is similar in the case of $^{76}Se$ but substantially smaller in the case of highly deformed $^{80}Sr$ compared to low energy spectroscopic measurements. In contrast the predominantly spherical nuclear shape seems to be maintained up to very high energies. The width however in the $^{80}Zr$ GDR is strongly increased, when compared to the ground state GDR (Fig. 2.6). Qualitatively this width can be explained with a deformation averaging over different nuclear shapes, weighting determined by the potential energy surface $E(\beta,\gamma,I,T)$,[4] where I is the angular momentum and T the nuclear temperature. The direct influence of angular momentum and Landau damping on the strength function seems to be negligible.

References:

1.  P. Carlos, et al., Nucl. Phys. A 258, 365 (1976); B.L. Berman and S.C. Fultz, Rev. Mod. Phys. 47, 713 (1975).
2.  M. Danos, Nucl. Phys. 5, 23 (1958).
3.  C.J. Lister et al., Phys. Ref. Lett. 49, 308 (1982).
4.  M. Gallardo, et al., Nucl. Phys. A 443, 415 (1985).
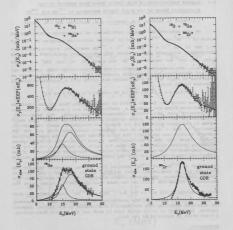
Fig. 2.6 Top box: γ-ray spectra from hot compound nuclei together with their best CASCADE fit. 2nd box: $\sigma_\gamma(E_\gamma)$ multiplied by $\exp(\alpha E_\gamma)$ with $\alpha^{-1}$=1.60 MeV for $^{76}$Se and $\alpha^{-1}$=1.71 MeV for $^{90}$Zr. 3rd box: Photoabsorption cross section $\sigma_{abs}(E_\gamma)$ inferred from the best fit to the excited state GDR. bottom box: Ground state photoabsorption data from (γ,n) reactions (Ref. 1).

## 2.7 Angular Distribution of High Energy Gamma Rays Emitted in the Statistical Decay of the Giant Dipole Resonance in $^{115}$Sb and $^{166}$Er

J.A. Behr, G. Feldman, C.A. Gossett, J.H. Gundlach, and K.A. Snover

We have measured the angular distribution of high energy $\gamma$ rays from the decays of $^{115}$Sb$^*$ and $^{166}$Er$^*$ formed at initial excitation energies of 54.2 and 49.2 MeV in the $^{12}$C + $^{103}$Rh and $^{12}$C + $^{154}$Sm reactions, respectively. The measurements were made with a large NaI spectrometer positioned at angles $\Theta_\gamma$=40, 90, 140$^\circ$ for decays of $^{115}$Sb$^*$ and $\Theta_\gamma$=40, 65, 90, 115, 140$^\circ$ for decays of $^{166}$Er$^*$. The measurement techniques and analysis of the high energy $\gamma$-ray spectral shapes have been previously presented (Ref. 1). The cross section as a function of angle and of $\gamma$-ray energy was fitted with a Legendre polynomial expansion of the form:

$$\sigma(\Theta,E_\gamma) = A_o(E_\gamma)(1 + a_1(E_\gamma)P_1(\cos\Theta) + a_2(E_\gamma)P_2(\cos\Theta)).$$

After correction for the effect of transformation from the laboratory to center-of-mass frame the measured $a_1$ coefficient at all $\gamma$ energies is found to be consistent with zero within experimental uncertainty. The measured $a_2$ coefficient as well as the $\gamma$-ray spectral shape are shown below. The solid curves in the upper portions of the figure are statistical model calculations described in Ref. 1 in which a two component Lorentzian form for the GDR strength function was required. The solid curves for $a_2$ in the lower portions of the figure are the predictions for dipole $\gamma$ emission from a system exhibiting prolate collective rotation for which one expects $a_2 \approx$-1/4 for the lower component of the split GDR and $a_2 \approx$+1/8 for the upper component. If one folds these two $a_2$ values in with the inferred photoabsorption cross section

for decays of $^{115}$Sb$^*$ and $^{166}$Er$^*$ obtained from the two component form for the GDR used in the statistical model analysis of the measured $\gamma$-ray spectral shapes, one obtains the curves shown in Fig. 2.7. The predictions are observed to follow the trend of the data from negative $a_2$ values below the mean GDR energy, $E_o \sim$15 and 14 MeV for $^{115}$Sb$^*$ and $^{166}$Er$^*$, respectively, to zero or positive values above $E_o$. The predictions do not however take into account the effect of averaging over the finite K distribution in the initial compound nucleus, the effect of which would tend to wash out the angular distribution, a trend which is suggested by the data.

References:

1. Nuclear Physics Laboratory Annual Report, University of Washington (1985) pp. 9, 11.

$^{12}C + {}^{154}Sm \rightarrow {}^{166}Er^*$  $\qquad$  $^{12}C + {}^{103}Rh \rightarrow {}^{115}Sb^*$
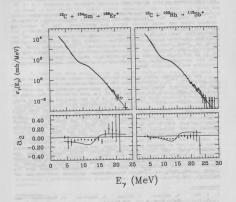
Fig. 2.7 Cross section and angular distribution coefficient $a_2$ from decays of $^{115}Sb^*$ and $^{166}Er^*$. Solid curves are as described in the text.

## 2.8 Statistical Decay of the Giant Dipole Resonance in $^{140}$Ce[*]

J.A. Behr, G. Feldman, <u>C.A. Gossett</u>, J.H. Gundlach, and K.A. Snover

We have measured continuum γ-ray spectral shapes from the decays of $^{140}$Ce formed at initial excitation energies of 58.7 and 70.0 MeV in the $^{18}$O + $^{122}$Sn reaction at E($^{18}$O)= 61.3 and 72.6 MeV. The nucleus $^{140}$Ce was chosen for study because it has a closed neutron shell at N=82 and is the heaviest compound nucleus we have formed with a closed shell.

The extremely low melting point of tin required a special preparation of the $^{122}$Sn target. The $^{122}$Sn target was prepared by evaporation on a thick Ta backing which was water cooled during the experiment. The $^{18}$O bombarding energies were sufficiently below the Coulomb barrier for $^{18}$O on Ta that the contribution from the Ta backing to the γ-ray yield was expected and was verified experimentally to be negligible. During the initial stages of the work we found that the isotopically enriched $^{122}$Sn material from ORNL contained light contaminants which were estimated to be in the mass range A ~ 23 to 28 and to be of order of few percent by weight. Special treatment of the tin material before the evaporation reduced the contamination to a tolerable and correctable level.

The statistical model analysis of the high energy γ-ray spectral shape for decay of $^{140}$Ce indicates that the excited state GDR strength function may be adequately described by a single component Lorentzian centered at E=14.5 MeV with width 7.6 MeV and 1.0 E1 sum rule strength. The width is significantly broader than the GDR width of 4.4 MeV observed in ground state photoabsorption studies[1] of $^{nat}$Ce and is consistent with our interpretation[2] that the increased GDR widths at high excitation in nuclei which have small static deformation reflect the distribution of finite deformation at finite temperature and spin in these nuclei. Similar to the results of a recent study (see Sec. 2.6) of the decays $^{90}$Zr, the only other closed shell nucleus studied in our laboratory, and unlike the case for any other nuclear with A>70, the GDR shape is well described by a single component resonance form. It appears that in the $^{90}$Zr and $^{140}$Ce nuclei the GDR at high excitation still seems to reflect an average spherical shape, and hence has a single component resonance shape, but that again the increased width signifies that the ensemble of states at temperature, T ~ 1.5 MeV, populated by the high energy gamma decay contains a distribution of finite deformation. In order to further test this hypothesis we plan to form a compound nucleus near the doubly closed shell at $^{208}$Pb in an experiment proposed for the LBL 88" cyclotron (see Sec. 2.11).

References:

1. H. Beil, R. Bergere, P. Carlos, A. Lepretre, A. Veyssiere, and A. Parlag, Nucl. Phys. A 172, 426 (1971).
2. Nuclear Physics Laboratory Annual Report, University of Washington (1985) p. 11 and Sec. 2.1 of this report.

## 2.9 High-Energy γ Rays from [3]He- and α-Induced Nonstatistical Reactions

J.A. Behr, G. Feldman, H.K. Glatzel, C.A. Gossett, J.H. Gundlach,
M. Kicinska-Habior, and K.A. Snover

We have continued our studies of high-energy γ rays from [3]He- and α-induced nonstatistical reactions. We have previously measured inclusive γ-ray spectra from [3]He- and α-induced reactions on a variety of targets (14≤A≤181) at 27 MeV bombarding energy. In all cases large continuous γ yields were observed in and above the giant dipole resonance (GDR) region (14 MeV≤E_γ≤30 MeV). The magnitude of these yields and their strong front-back asymmetry cannot be explained by a statistical emission process.

We have since measured an angular distribution of γ rays from 27 MeV α+[95]Mo. The front-back asymmetry observed is intermediate between that measured for targets [46]Ti (Ref. 2) and [15]Sm, consistent with systematics of the total γ-ray yields relating the α-induced nonstatistical reactions to target mass. Possible spectrum distortions due to summing of γ rays in the detector and contributions at high E_γ from light contaminants in the Sn and Mo targets were experimentally checked and found to be negligible.

We have now done calculations of direct radiative capture as well as capture through semidirect excitation of the GDR in the target for the target [124]Sn. Direct radiative capture has a relatively flat γ-ray spectrum compared to the data for both projectiles, giving too little yield near the GDR and ≈10 times too much yield at high E_γ. The γ-ray yield from semidirect excitation of the target GDR is small with respect to direct capture for both projectiles. Using the same semidirect formalism, we have estimated the radiation from decay of the GDR excited in the projectile. For [3]He this process is of the same magnitude as the semidirect target excitation and thus is negligible. For [4]He (whose excitation by an N≠Z target is not isospin-forbidden), this process gives yields approaching those from direct radiative capture; for both [4]He and [3]He this process interferes destructively with direct emission.

Though the angular distributions from the direct-semidirect calculations are qualitatively similar to those observed, the calculated flat spectrum shapes are markedly different from the observed spectra. The measured spectra fall exponentially with E_γ, qualitatively consistent with statistical-like decay but with an effective temperature of order twice the actual temperature, suggesting a pre-equilibrium process more complicated than direct-semidirect emission.

### References:

1. Nuclear Physics Laboratory Annual Report, University of Washington (1985) p. 15, 22.

2. Nuclear Physics Laboratory Annual Report, University of Washington (1985) p. 22.

3. N. Shikazono and T. Terasawa, Nucl. Phys. A 250, 260 (1975).

## 2.10 Nucleon Decay of the Ground-State GDR in the Schematic Model

J.A. Behr, G. Feldman, and K.A. Snover

In an earlier publication,[1] we have reported a definite correlation between GDR $(\gamma, p_0)$ strength (obtained from $(p, \gamma)$ measurements by detailed balance) and spectroscopic strength. This relation can be simply understood by a schematic model calculation including the GDR, with the extreme approximation of equal barrier penetrability for all nucleon decay channels.[2]

We are now improving these calculations by relaxing the extreme limit of equal penetrabilities stated above. This is a continuation of work reported in an earlier Annual Report.[3] In the schematic model, the GDR is represented by a coherent sum of 1p-1h excitations (built on the ground state in this case, or in general, on an excited state) in which the amplitude for each term is just given by the E1 matrix element for the single-particle transition between shell model orbits $n'\ell'j'$ and $n\ell j$ (computed in a simple harmonic oscillator basis). The subsequent decay of the excited particle into the continuum is determined by integrating over the GDR photoabsorption cross section, accounting for the Coulomb and centrifugal barrier effects at each energy step in the integration procedure. The overlap between the initial state (particle-hole configuration) and the final state (continuum particle + residual hole state) is given by spectroscopic factors.

As a test of the improved calculation, we have applied the model to several cases in light nuclei ($^{16}$O, $^{28}$Si, $^{40}$Ca) for which particle decay branching ratios of the ground-state GDR can be found in the literature. In all of the cases, the improved schematic model calculation gives better agreement with the experimental data than the extreme emission model. The case of $^{40}$Ca is shown in Fig. 2.10. The notable features are the relative enhancement of the proton decay strength to the lowest two states in $^{39}$K (especially the $\ell = 0$ first excited state) and the compensating inhibition of decays to higher-lying states ($E_x > 5$ MeV).

Having gained confidence in the ability of these schematic model calculations to correctly reproduce nucleon decay strengths of the ground-state GDR, we plan to apply the model to our recent experimental results obtained in $(p, \gamma)$ capture reactions to excited final states (see Sec. 2.2).

References:

1. D.H. Dowell, G. Feldman, K.A. Snover, A.M. Sandorfi and M.T. Collins, Phys. Rev. Lett. 50, 1191 (1983).
2. K.A. Snover, Journal de Physique 45, C4-337 (1984).
3. Nuclear Physics Laboratory Annual Report, University of Washington (1984), p. 7.
4. D. Brajnik et al., Phys. Rev. C 9, 1901 (1974).
5. H. Ullrich and H. Krauth, Nucl. Phys. A 123, 641 (1969).
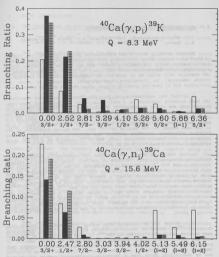
Fig. 2.10  Comparison of schematic model calculations for GDR nucleon decay branching ratios vs. the experimental data of Brajnik[4] and Ullrich.[5] The open bars (left side) indicate the calculated branching ratio in the extreme limit of equal barrier penetration for all nucleon decay channels. The patterned bars (right side) represent the result from the improved calculation, including effects due to penetrability. The empirical data are shown by the solid bars in the middle.

## 2.11 Nuclear Structure at Elevated Temperature

J.A. Behr, C.A. Gossett, J.H. Gundlach, K.T. Lesko,[*] E.B. Norman,[*] and K.A. Snover

We have recently begun a new experimental program to extend our studies of the high energy γ decay from highly excited compound nuclei formed in heavy ion collisions to the qualitatively higher spin and nuclear temperature regime accessible at the Lawrence Berkeley Laboratory 88" cyclotron. Measurements at LBL energies will allow us to form heavier compound nuclei than possible at tandem energies, to investigate nonstatistical processes in heavy ion collisions and to look for possible nuclear shape changes at high excitation.

A 10"×10" NaI spectrometer on loan from Lawrence Livermore Laboratory has been recently installed on a newly constructed low background beam-line. We must know the energy dependence of the efficiency and lineshape response of the detector for folding in with a statistical model analysis of the γ-ray spectral shapes. In our first run at LBL we studied the detector response and found the energy resolution at 22.6 MeV to be 6.5% FWHM compared with ~ 3.3% at the same energy for the Seattle 10"×10" NaI. The energy dependence of the detector efficiency including geometry and shielding effects was measured relative to the Seattle detector using the p+$^{11}$B reaction at $E_p$=7 MeV which produces discrete lines from 2 to 22 MeV.

During the first run we also studied the experimental feasibility of performing measurements with $^{12}$C beams at 200 MeV. From our tests we believe that for a 200 MeV $^{12}$C beam cleanly transported to the target, by using the time structure of the cyclotron beam and time of flight techniques, we are able to cleanly distinguish prompt γ events from the target from neutron induced events from the target and from other sources of background. Very preliminary results from short test runs of 200 MeV $^{12}$C on $^{96}$Mo and $^{nat}$Ta targets indicate measured γ-ray spectra which exhibit a bump near the GDR energy and which extend to $E_\gamma$ ~ 50-60 MeV. In each case the γ-ray yield at $E_\gamma$=40 MeV is of order of a few μb/MeV. Much further analysis is required in order to provide quantitative understanding of the origin of the observed high energy γ yield.

In a second run we measured high energy γ-ray spectral shapes from decays of $^{164}$Er formed at initial excitation energies of 70 and 105 MeV and mean initial spins of 26 and 29ℏ in the $^{12}$C + $^{152}$Sm reaction for E($^{12}$C) = 84 and 121 MeV, respectively. Although the analysis of these results is presently only in the initial stages, very preliminary analysis suggests that the high energy γ yield from measurements at E($^{12}$C)=84 MeV can be accounted for by statistical decay from a thermally equilibrated system, while that measured at 121 MeV seems to be in excess of that expected from a statistical model calculation.

### Reference:

* Lawrence Berkeley Laboratory, Berkeley, CA 94720.

3.  HEAVY ION REACTIONS

3.1  The Calibration of Sub-Coulomb Heavy Ion Proton Transfer Reactions

K.J. Davis,[*] S. Gil,[*] M.A. Khandaker, A.J. Lazzarini,[†] D.D. Leach,
R.A. Loveman, T. Murakami, and J.L. Osborne

The reaction cross section for the transfer of a proton between heavy ions involves the spectroscopic factor and square of the radial wave function of the transferred proton in the both the initial and final nucleus. These quantities can be isolated for a particular configuration by measuring a reaction triad, such as the one given below.

A.  $^{89}Y(^{15}N,^{16}O)^{88}Sr$

B.  $^{89}Y(^{27}Al,^{26}Si)^{90}Sr$

C.  $^{16}O(^{27}Al,^{26}Si)^{15}N$

The successful measurement of these reactions as well as the elastic scattering in the entrance and exit channels was reported in last year's Annual Report.[1] Over the course of the past year all of the experimental data has been analyzed to determine the absolute transfer and elastic scattering cross sections.

In order to extract information about spectroscopic factors and radial wave functions the experimental transfer cross sections need to be related to calculated values. The transfer cross sections have been computed using the finite range DWBA code LOLA[2] under the assumption that all of the spectroscopic factors are unity. In principle, then, the products of the spectroscopic factors would be given by the ratio of the measured cross sections to the computed values. This procedure is complicated by the sensitivity of the calculations to the choice of proton binding well parameters. It has been shown, however, that the spectroscopic factors times the square of the radial wave functions evaluated at a "match center" radius can be determined with very little sensitivity to the choice of these parameters.[3] There is additional model dependence in the calculation arising from the choice of parameters used to describe the ion-ion interaction in the entrance and exit channels. We have tried to minimize this by choosing parameters which account for the observed elastic scattering.

Some remaining problems, still under investigation, are discrepancies between calculations performed in the post and prior representations and differences between experiment and theoretical predictions of the shape of the excitation function in the vicinity of the Coulomb barrier.

References:

*   Comision Nacional de Energia Atomica, Buenos Aires, Argentina.
†   Kaman Instrumentation, Colorado Springs, CO 80933.
+   University of Colorado, Boulder, CO 80309.
1.  Nuclear Physics Laboratory Annual Report, University of Washington (1983) p. 28.
2.  R.M. DeVries, Phys. Rev. C 8, 951 (1973).
3.  K.G. Nair et al., Phys. Rev. C 8, 1129 (1973).

## 3.2 Spin Distributions in Sub-Barrier Heavy Ion Fusion

D.D. Leach,   T. Murakami,   M.J. Murphy,   A. Ray,   C.-C. Sahm,   and R. Vandenbosch.

We have continued our study of fission fragment angular distributions as a probe of the mean-square spin values in heavy-ion-induced sub-barrier fusion. Previously[1] we reported on the $^{12}C+^{236}U$ and $^{16}O+^{232}Th$ reactions, where we observed mean-square spin values which were typically twice as large as expected from current theoretical models. As both $^{236}U$ and $^{232}Th$ are strongly deformed nuclei, we decided to see if the discrepancy persisted when the target nucleus is spherical. We studied the reaction $^{16}O+^{208}Pb$. As expected, the sub-barrier fusion excitation function for this target falls much more steeply with decreasing bombarding energy. This excitation function had the shape expected from theoretical models, but again the anisotropies and hence the mean-square spin values were larger than expected. A summary of the results of all three systems is shown in Fig. 3.2.

The $^{16}O+^{208}Pb$ system is particularly interesting because two unusually complete coupled channels calculations have been performed for this system.[2,3] These calculations include both the inelastic and transfer channels explicitly, so that no imaginary potential is necessary. When the potential strength is adjusted to simultaneously reproduce the elastic scattering and the fusion cross section, and the transfer coupling strength to reproduce measured excitation functions, the mean-square spin values predicted still fall short of expectations at all but the lowest bombarding energy. We do not understand the origin of this discrepancy. One assumption which bears further investigation is the use of the reduced mass for the inertial mass in the quantum-mechanical tunnelling calculations.

References:

1.  R. Vandenbosch, T. Murakami, C.-C. Sahm, D.D. Leach, A. Ray, and M.J. Murphy, Phys. Rev. Lett. 56 1161 (1986).

2.  I.J. Thompson, M.A. Nagarajan, J.S. Lilley, and B.R. Fulton, Phys. Lett. B 157, 210 (1985).

3.  S.C. Pieper, M.J. Rhoades-Brown, and S. Landowne, Phys. Lett. B 162, 43 (1985).
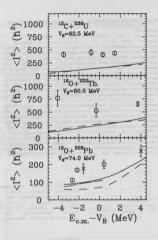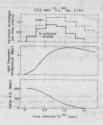
Fig. 3.2 Comparison of mean-square spin values deduced from fission fragment anisotropies with different models. The full curve and dashed curves are based on the Esbensen and Wong models. The dashed-dot curve is from the coupled channels calculations of Pieper et al.

## 3.3    Pre-Equilibrium Nucleon Emission in Heavy Ion Fusion Reactions

R. Vandenbosch

We reported last year[1] on a calculation of several quantities characteristic of pre-equilibrium neutron emission. Our starting point was the dynamical model of Randrup[2] which incorporates dissipation based on the exchange of nucleons. This model has been very successful in accounting for a broad range of phenomena (fusion probabilities, energy damping and angular momentum transport, Z and A distributions in quasi and deeply inelastic scattering) at low bombarding energies. We found that by keeping track of the exchange rates as a function of relative kinetic energy and correcting for the fraction of transfers to bound states one could understand the bombarding energy dependence of the pre-equilibrium neutron multiplicity and especially the observations of average source velocities of about 1/2 the beam velocity.

The present calculation was motivated by a recent report[3] that at 25 MeV/A $^{12}$C bombardment of $^{158}$Gd the pre-equilibrium component could best be parameterized by a source which had a fairly high temperature. Since our previous calculation showed pre-equilibrium emission occurring on the average after considerable energy damping, we decided to investigate this question more quantitatively. The results of a typical trajectory are given in Fig. 3.3. One sees from this figure that at the most probable time for pre-equilibrium emission the projectile-like fragment has achieved a high temperature. This trajectory eventually leads to incomplete fusion. The calculation also reproduces the average source velocity observed in this reaction.



Fig. 3.3.  Time dependence of neutron exchange rate, light-fragment temperature and radial kinetic energy in a typical collision leading to incomplete fusion accompanied by pre-equilibrium neutron emission.

## References:

1.  Nuclear Physics Laboratory Annual Report, University of Washington (1986) p. 26.
2.  J. Randrup, Nucl. Phys. A 327, 490 (1979).
3.  E. Holub et al., Phys. Rev. C 33, 143 (1986).

## 3.4 Mean Spin of $^{28}$Si Produced by Decay of Orbiting Complex

D.D. Leach, K.T. Lesko, A. Ray, D. Shapira,$^*$ and R. Vandenbosch

We have completed our study of the "orbiting" decay channels in the $^{28}$Si+$^{12}$C reaction. We have performed coincidence studies using reverse kinematics and detection of $^{12}$C at 0° (corresponding to 180° inelastic scattering). The results of the $^{12}$C-4.43 Mev gamma correlation experiment were reported last year. During the same experiment we also measured the yields of coincident protons and alphas. The purpose of this measurement was to use the well-known enhancement of the alpha-to-proton yield ratio with increasing spin to deduce the average spin of the $^{28}$Si partner to the $^{12}$C detected at 0°. We have determined the angle-integrated alpha/proton ratio for the Q-value range (−30<Q<−20) MeV from the energy spectra at three angles for 142.7 MeV $^{28}$Si on $^{12}$C. We then performed statistical model calculations of the proton and alpha yields, corrected for the experimental energy thresholds, as a function of excitation energy and mean spin. (A gaussian spin distribution with unit dispersion was assumed.) The experimental $^{12}$C singles Q-values spectrum was used to perform the weighted sum over excitation energy. The resulting dependence on spin is compared with the experimental ratio in Fig. 3.4, from which we deduce an average spin of 8.7+0.7. There is an additional uncertainty of perhaps 15% from the statistical model calculations and the Q-spectrum weighting. This spin value is consistent with complete damping of the entrance channel orbital angular momentum into rigid rotation of an extended dinuclear complex.
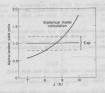


Fig. 3.4 Comparison of experimental alpha-to-proton yield ratio with J-dependence of statistical model calculation.

References:

*   Physics Division, Oak Ridge National Laboratory, Oak Ridge, TN 37830.

1.  Nuclear Physics Laboratory Annual Report, University of Washington, (1985) p. 31.

2.  A. Ray, Ph.D. Thesis, University of Washington, 1986.

3.5 Total Reaction Cross Section for $^{12}C$ on $^{12}C$, $^{40}Ca$, $^{90}Zr$ and $^{208}Pb$ between 10 and 35 MeV/A

J.G. Cramer, A.J. Lazzarini,[*] D.D. Leach, R.A. Loveman,[†] W.G. Lynch,[+]
T. Murakami,[+] C.C. Sahm,[x] D.R. Tieger, M.-Y. Tsang,[+] and
J. Van der Plicht[$]

At low collision energies the total reaction cross section between heavy ions is primarily determined by the collective nuclear behaviour. At higher collision energies the individual collisions of nucleons in the target with those in the projectile may assume more and more prominence. In the Glauber model[1] the total reaction cross section arises from the scattering of a single nucleon in the projectile from a single nucleon in the target. In this model, the rapid decrease of the nucleon-nucleon cross section with increasing energy leads to a minimum in the total reaction cross section at about 300 MeV/nucleon. For the carbon on carbon reaction, a large body of available data supports this simple model.

In 1985 we continued our experimental program to measure the energy dependence of the heavy ion total reaction cross section of heavier systems with an experiment which investigated the reactions $^{12}C$:$^{12}C$, $^{40}Ca$, $^{90}Zr$ and $^{208}Pb$ at 10, 15, 25 and 35 MeV/nucleon. Like in the first experiment[2] the S-320 spectrometer at the NSCL was used to measure elastic scattering angular distributions. The total reaction cross sections were determined by an optical model analysis using a Woods Saxon potential for the real and the imaginary part of the optical potential.

During the course of the evaluation of the 1985 experiment a subtle normalization error was discovered which affects the 1984 data for the carbon on zirconium system. Therefore, for this reaction, only the 1985 data were used for the optical model analysis.

In Fig. 3.5 the results of this work (symbols) are shown together with the predictions of the Glauber model (solid curves). The data at 83 MeV/nucleon are taken from Ref. 3. The total reaction cross sections determined with this method agree remarkably well with the predictions of the Glauber model.

References:

* Present address: Kaman Instrumentation, 1500 Garden of the Gods Road, P.O. Box 7463, Colorado Springs, CO 80933.
† Nuclear Physics Laboratory, Box #446, University of Colorado, Boulder, CO 80309.
+ National Superconducting Cyclotron Laboratory, Michigan State University, East Lansing, MI 48824.
x Present address: Gesellschaft für Schwerionenforschung, GSI, Postfach 11 05 41, 6100 Darmstadt, Fed. Rep. Germany.
$ Laboratory for Nuclear Science, Massachusetts Institute of Technology, Cambridge, MA 02139.

1.  Nuclear Physics Laboratory Annual Report University of Washington (1985) p. 33.
2.  R.M DeVries et al., Phys. Rev. C 22, 1055 (1980).
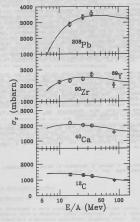3.  S. Kox et al., Nucl. Phys. A 420, 162 (1984).

Fig. 3.5 Summary of total reaction cross section data. The solid curves are the predictions of the Glauber model.

### 3.6 Sub-barrier Elastic and Inelastic $^{16}$O Scattering from $^{148}$Sm

K.J. Davis, M.A. Khandaker, T. Murakami, D.P. Rosenzweig, and C.-C. Sahm

Considerable interest has recently been given to reactions between two complex particles at energies near the Coulomb barrier. In the fusion cross sections at sub-barrier energies, an appreciable enhancement has been observed over the values predicted on the basis of simple barrier penetration. For elastic scattering at these energies, the usual folding optical potential has an unresolved normalization problem. The standard explanation for the origin of the enhanced yield is the target deformation and especially the coupling to quasi-elastic transfer processes. In order to understand the interplay among elastic scattering, inelastic scattering (deformation of target nucleus), single nucleon transfer, and the fusion reaction we measured the elastic and inelastic scattering of $^{16}$O from $^{148}$Sm at sub-barrier energies. The fusion reaction of this system has already been measured by Stokstad et al. with good accuracy.[1]

The experiments were performed with 60.02, 62.53 and 65.04 MeV $^{16}$O$^{+8}$ beams. These energies were chosen so that the energies at the center of target would be the same energies as in the reported fusion study of this system.[1] A $^{148}$Sm target of about 20 $\mu$g/cm$^2$ thickness backed by a $\approx$20$\mu$g/cm$^2$ carbon foil was used. The beam direction and intensity were monitored by a pair of detectors at $\pm$20.00 $\pm$0.04°. The angular distributions were measured by four silicon surface barrier detectors of 150-300 $\mu$m thickness. The absolute cross sections were determined by normalizing to Rutherford scattering using the monitor counters.

The preliminary analysis shows that at least in this system the single nucleon transfer channels do not play an important role compared with the inelastic channels. Even at the our lowest energy the 2$^+$ and unresolved 4$^+$ states were strongly populated. The analysis using a coupled-channels formalism is in progress.

#### Reference:

1.  R.G. Stokstad, Y. Eisen, S. Kaplanis, D. Pelte, U. Smilansky, and
    I. Tserruya, Phys. Rev. C 21, 2427 (1980).

4.    FUNDAMENTAL SYMMETRIES IN NUCLEI: $0^+ - 0^-$ ISOSCALAR PARITY MIXING IN $^{14}$N

### 4.1    Apparatus Development

#### E.G. Adelberger, H.E. Swanson, and V.J. Zeps

Because our polarized ion source is not yet producing beam, we have
entered a collaboration with W. Haeberli, J. Sromicki, and P. Quin at the
University of Wisconsin and moved our apparatus to the Wisconsin tandems. This
was practical since we had developed a powerful, portable data acquisition
system (see Sec. 4.2). In order to control precisely the direction of the
proton polarization we developed a computer control system for the Wien spin
precessor. This system allows our data acquisition computer to set the
rotation angles and precision of the Wien. The system is optically isolated
to avoid ground loops and uses a Hall probe gauss meter to set the B field,
and inexpensive commercial PMT bias supplies to set the E field. This system
has proved to be very stable and extremely convenient.

In order to obtain an emittance figure for the target beam-spot which is
more symmetrical in the horizontal and vertical directions we have added a
third quadrupole element to the final quadrupole doublet. This resulting
quadrupole triplet gives us enough freedom to form the symmetrical beam spot
that we expect is required to minimize systematic errors due to residual
transverse components of the proton polarization.

We have continued to make improvements in the rest of the apparatus.
For example we increased the gain and dynamic range of our wide-band beam
stabilization system by substituting higher capacity commercial bipolar power
supplies for home-built units and by relocating one of the ferrite-core
steerer magnets. We have also added a set of electrically isolated slits at
the entrance and exit of our quadrupole triplet to give a better monitor of
the beam-tuning.

\*\*\*\*\*\*

### 4.2    New Data Acquisition System

#### E.G. Adelberger and H.E. Swanson

We have developed a very powerful data acquisition system based on an
IBM PC-AT computer with a TRANSIAC CAMAC interface, plus a DATA TRANSLATION
D/A and D/D board and a Hercules monochrome graphics card. The system runs
under DOS 3.0 and is written in IBM Professional Fortran with a few crucial
assembler subroutines. The system reads and controls the 48 CAMAC scalers,
reads the Wien E and B fields, and the x and y coordinates of the target
position via A/D's, controls the Wien precessor and the target position
scanner, and provides us with a comprehensive real-time analysis of the data.

All raw data is written on floppy discs for a permanent record. An IBM Proprinter gives us graphics and text hardcopy (an example of this output is shown in Sec. 4.4).

Our system has proven to be extraordinarily effective. We can see correlation between any two of 48 different quantities (asymmetries, rates, precessor quantities, etc.), obtain excitation functions of any of these 48 quantities, or execute complicated algorithms which find the effective center of our apparatus or measure the profiles of the intensity and transverse polarization of the beam on target. It also allows us to set the spin on target in an arbitrary direction merely by typing in the desired polar coordinates of the target polarization vector and then to control the spin via a digital feedback loop. This loop is very effective. For example, it maintains the mean spin of a nominally longitudinally polarized beam to with~ 0.1° of the desired direction. As a result corrections to our longitudinal analyzing powers due to misalignments of the mean polarization are negligible.

\*\*\*\*\*\*

## 4.3   Strip Target Beam Analyzer

E.G. Adelberger, H.E. Swanson, and V.J. Zeps

A strip target beam analyser has been built into the data aquisition system. It measures the intensity profile of the beam and any transverse polarization moments as a function of position across the beam. To obtain moments of the beam, the program automatically steps a strip target through the beam using the remote target positioning system. We have added optical shaft encoders and an interface to provide the actual target position for the computer. At each target position, the yields from all eight counters and the x and y positions are obtained. The computer then calculates the transverse asymmetries and displays them along with the counting rates for each target position. We have purchased an IBM Proprinter to obtain a hardcopy of these and other plots generated by the aquisition system. An example of one of these plots is shown in Fig. 4.4.

Strip targets were made by evaporating approximately 100 $\mu g/cm^2$ natural carbon in 0.3 mm wide strips on a thin carbon backing. (This is described in more detail in Sec. 12.1.1 of this report.) At an energy $E_x$ approximately 1.73 MeV (near the $3/2^+$ resonance in $^{13}N$ $E_x=3.54$ MeV) the transverse analyzing power in the back detectors about 0.8. We have calculated the effect of the width of the strip on the measurement of the FWHM of the beam. A strip equal in width to the FWHM of the beam increases the measured width by only about 25 percent. Since the measured FWHM's are between 1 and 1.5 mm, we could use even wider strips in order to increase the counting rates.

\*\*\*\*\*\*

## 4.4    Study of Systematic Errors Using Polarized Beam

E.G. Adelberger, C.A. Gossett, W. Haeberli, P. Quin, J. Sromicki,
H.E. Swanson, and V.J. Zeps

Since moving to the Wisconsin tandem, we have studied systematic effects associated with a polarized beam. All of the effects we had previously studied with unpolarized beam[1] have been eliminated as possible sources of a substantial false asymmetry. On the other hand, false asymmetries due to spin effects have been shown to be critical.

We developed a program that calculates the expected countrate in each detector for any set of beam parameters (mean position and width, beamspot size and divergence, and polarization profile) given the angular distributions of cross-section and transverse spin analyzing power. Our model accurately describes the measured detector sensitivities to differences in beam parameters for the two spin states.

We have set an upper limit of $<5\times10^{-4}$ mm on position modulation of the beam using a gold target ($A_y\cong0$). This corresponds to a false $A_z$(back-front)$\times1\times10^{-8}$. Strip target measurements (see Sec. 4.3) allow us to set limits on "breathing mode" modulation of the beam. A difference in beam width of $<0.2\%$ between spin states has been measured, yielding a false $A_z$(b-f)$<1.5\times10^{-8}$, which is negligible compared to the expected PNC signal of $A_z$(b-f)$\cong2.5\times10^{-7}$. Energy modulations have been investigated using the narrow $^{13}$C(p,γ) resonance at $E_p\cong1.75$ MeV. An upper limit of $\Delta E_p\cong0.3\pm0.6$ eV was measured. Because of the sharp dependence of the cross-section on energy, our sensitivity to energy modulation can be as large as $dA_z$(b-f)/$dE\cong1\times10^{-7}$/eV. If we choose to lose 20% of the PNC signal by a slight shift in energy ($\Delta E_p\cong1.5$ keV), we can make this sensitivity negligible. This optimum energy[2] determined by modulating the target voltage by $\pm30$V and measuring $A_z$(b-f) vs. $E_p$.

The dominant source of potential false asymmetries are from transverse spin effects. This false asymmetry can be expressed as

$$A_z^{fake}(b-f) = A_0(\overline{e\times p})\cdot z + B_0\overline{\alpha\cdot p}$$
$$+ A_1(\Gamma_x^s \partial p_z/\partial x - \Gamma_y^s \partial p_z/\partial y) + B_1(\Gamma_x^z \partial p_z/\partial\alpha_x + \Gamma_y^z \partial p_z/\partial\alpha_y),$$

where $\overline{p}$ = polarization vector,

$\overline{e}$ = displacement of beam on target from nominal chamber axis,

$\overline{\alpha}$ = angle of beam on target from nominal chamber axis,

$\Gamma_i$ = FWHM of beam w.r.t. the ith phase space parameter.

The first term in the expression vanishes if the beam is centered in the chamber, and the mean transverse polarization is locked to zero. Using the sensitivity of $A_z$ to the beam position and angle, we determined the central axis of the chamber with a transverse polarized beam. Consequently, contributions from the first term can be kept to a level of $<5\times10^{-8}$. The

31

second term in this expression leads to the dominant false asymmetry for this experiment. As shown in Fig. 4.4, the polarization direction is not uniform. These gradients are not fully understood, but appear to be introduced at the spin processor. As it stands, these "circulating" transverse polarization moments can contribute a false $A_z(b-f) \leq 1 \times 10^{-7}$, which is 40% of expected PNC effect. We have observed that the "circulating" moments can be substantially changed with source and L.E. tuning, yet are stable over several hours when minimal tuning is done. More tests will be performed to pinpoint the source of (and cure for) these moments. We hope to take real data this summer.

References:

* University of Wisconsin, Madison, WI 53706.
1. Nuclear Physics Laboratory Annual Report, University of Washington (1985) p. 39.
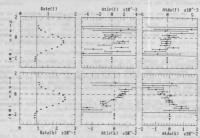


Fig. 4.4 Shown are rates and asymmetries for front and back detectors vs. strip target position (see Sec. 4.3). The rates are shown with a line depicting the average background, corresponding to 30-40% of the peak rate. A linear fit to the asymmetries is performed and displayed to determine the 1st polarization moment. Since Atlr $\propto$ P$_y$, Atdu $\propto$ P$_x$, it is the slope $\partial(\text{Atdu})/\partial y$ that leads to a false $A_z(b-f)$ signal. $A_z(\text{front})=.02$, $A_z(\text{back})=.80$, consequently 0 slope is measured for the front detector asymmetries. This plot was produced on an IBM Proprinter by our on-line analysis program.

32

5.    SEARCH FOR AN INTERMEDIATE RANGE FORCE COUPLED TO BARYON NUMBER

E.G. Adelberger, B. Heckel, J.H. Gundlach, T.J. Irwin, K.D. McMurry, P.J. Raab, C.W. Stubbs, and H.E. Swanson

## 5.1   Basic Idea

A recent reanalysis[1] of the data from Eotvos' classic torsion balance experiment has raised the possibility of an intermediate range force coupled to Baryon number. Furthermore, the discrepancies between geophysical and laboratory determinations of Newton's gravitational constant G are not inconsistent with the existence of such a force. The more recent precise tests of the Equivalence Principle done by Dicke and Braginskii would not have been sensitive to forces which couple to Baryon number and which have a range large compared to laboratory dimensions but much less than 1 Astronomical Unit.

We have begun an experiment to search for an intermediate range force which couples to Baryon number. The basic idea is to do a "mountaineer's" version of the Eotvos experiment: a torsion balance experiment placed beside a cliff should allow an angular deflection if test masses of different B/M (baryon number/mass) experienced a medium-range force proportional to B. This deflection would arise when the gravitational force on a test mass is not aligned with the force vector from a B-dependent force. The medium-range nature of the new force means that its direction and magnitude are sensitive to the local mass distribution. By selecting masses with large differences in B/M and by performing the experiment at a site with suitable topography, we should see an effect much larger than that claimed for the original Eotvos data. Rotations as large as a fraction of a milliradian are possible.

Since the experiment requires us to determine the angular equilibrium position of the torsion pendulum, we propose to rotate the entire apparatus in a horizontal plane and to monitor any change in the system's equilibrium position. The signature of the new force would be unique in its phase and frequency characteristics, and can be distinguished from gravity gradient effects. Checks for systematic errors can be made by performing the experiment with masses of equal B/M.

## References:

*    Physics Department, University of Washington.
1.   E. Fishbach, et al., Phys. Rev. Lett. 56, 1 (1986).

******

33

The development of the apparatus needed to search for any medium range force which couples to Baryon number is now well under way. We have decided upon a four-mass torsion pendulum suspended from a fiber 1 meter in length. The test masses are surrounded by cylindrical electrostatic and magnetic shields. The masses, fiber and shields are inside a vacuum chamber which sits atop a bearing which is in turn supported by a passive vibration isolation system. The angular position of the masses is measured with an optical lever system. Thermistors measure the temperature at appropriate points in the system.

The four masses are supported by a quartz holder, at the four corners of a square 6 cm on a side. The holder also supports mirrors used for the readout system. The four-mass configuration is less sensitive to gravitational gradients than a two-mass system would be. At present each of the four masses is a 10 gm Aluminium cylinder. Eventually these will be replaced with K masses and two LiH masses, all encapsulated in Cu.

We measure the angular position of the test masses, and so it is advantageous to use fibers with small torsion constants. Work is proceeding with Tungsten fibers roughly 1 micron in diameter. The aluminium test masses have a period of 346 seconds when suspended from the 1 micron fiber. The modular design of the apparatus allows rapid changing of both fibers and test masses. Quartz fibers may well be used in the final version. The upper end of the fiber is attached to a 50mm non-rotating micrometer drive, with a vacuum feedthrough. The micrometer is mounted on a rotational stage. This allows us to position the test masses in the vertical direction, and to change the orientation of the test mass system relative to the vacuum chamber. We are currently working on an optical position detection system which will determine the position of the fiber inside the vacuum can. This will allow us to insure that rotating the apparatus does not affect the position of the test mass inside the can.

The optical lever is driven by a modulated LED which launches a collimated beam downwards through a quartz window into the vacuum chamber. The beam is rotated into the horizontal plane by a pentaprism and is reflected off of the mirror on the test mass holder. This returning beam also passes through the pentaprism, and up through the detection optics to be focussed onto a lateral-effect photodiode. The optical system is designed to be sensitive to angular displacements at the microradian level. The output of the photodetector electronics reflects the location of the test masses. This signal is digitized at 13 bits. The data acquisition electronics are all CMOS, allowing battery powered operation.

We hope to be making measurements in the near future.

## 6.1   Precision Measurement of the Antiproton Mass: A Test of CPT Invariance[1]

G. Gabrielse,[*] H. Kalinowsky,[†] W. Kells,[+] and T.A. Trainor[+]

We are preparing to measure the mass of the antiproton to 1 part in $10^9$ at the LEAR facility at CERN. A comparison of this mass with that of the proton would serve as a unique test of CPT invariance for baryons (now tested to ~ $1/10^4$.[2] The antiproton mass will be measured from the cyclotron frequency of a single antiproton caught in a precison Penning trap.

A principal experimental difficulty is the reduction of the energy of the LEAR antiprotons from their present minimum ( ~ 21 MeV) to a trappable energy ( ~ 1 keV). A beryllium foil will degrade the antiprotons and send them into a suitable solid angle to be caught in a simple cylindrical "catcher" trap from which they can be transferred to the precision trap. The LEAR storage ring typically contains $5 \times 10^9$ antiprotons, and these may be extracted either in a steady stream ($10^4$-$10^5$/s) or in compressed bunches.

Progress has been made on several fronts. Using a duoplasmatron ion source we have demonstrated trapping of monoenergetic 1 keV protons in a version of the cylindrical trap. At the NPL we have i) used 5 and 16 MeV proton beams to study the energy and angular distributions of nearly stopped protons in beryllium (sec. 6.2), ii) used 16-18 MeV proton beams to develop a time-of-flight technique with which to maximize and measure the yield of 1 keV protons from a degrader (sec. 6.3) and iii) used an 18 MeV chopped proton beam (10 μs bunches 10 ms apart) to develop the fast electronics and diagnostics for the catcher trap.

At CERN (May 1986) we used the time-of-flight technique and steady extraction to observe 1 keV antiproton yields transmitted by a Be degrader. We also tested the catcher trap system using bunched extraction.

The signature for successful trapping is detection of annihilation pions well after the beam pulse has passed and coincident with opening the trap. We found that the pion detectors (plastic scintillators) were saturated by the beam pulse and were not sufficiently recovered at the end of the trapping period to provide an unambiguous trapping signal. The pion detectors are being modified to gate off the phototubes during the beam pulse.

References:

*   Department of Physics, University of Washington.
†   University of Mainz, Federal Republic of Germany.
+   Fermi National Accelerator Laboratory, Batavia, IL 60510.
1.  "Precision Comparison of Antiproton and Proton Masses in a Penning Trap," Proposal P83 to the Proton Synchrotron Coordination Committee of CERN, Geneva, Switzerland (April 15, 1985).
2.  Particle Data Group, Rev. Mod. Phys. 56, No. 2, Part II, S37 (1984).

## 6.2 Angle and Energy Distributions of 5 and 16 MeV Protons Nearly Stopped in Beryllium

J.R. Olson, J.C. Sandberg,* and T.A. Trainor

Our program to measure very precisely the antiproton mass in a Penning trap requires "brute-force" slowing of 21 MeV antiprotons to 1 keV in a beryllium degrader foil. Several design aspects of the trapping experiment require detailed information on the energy loss process. We have used a proton beam to model the process with the assumption that protons and antiprotons behave similarly down to energies of order 1 keV, an assumption that is confirmed by results at CERN reported below (see Sec. 6.3).

A primary beam of 5 or 16 MeV protons was scattered from a 100 $\mu g/cm^2$ gold foil and collimated to provide a secondary beam of $10^{-5}$ particles/sec. This beam was incident on beryllium foils 0.25 mm thick (5 MeV) or 1.75 mm thick (16 MeV). A monitor detector was placed symmetrically on the other side of the primary beam to intercept the same number of protons as the beryllium foil and thus serve as a normalization.

Particles transmitted by the beryllium foils were detected by an array of solid-state counters placed every 5° from 0° to 25° or by a single counter placed very close to the beryllium which intercepted essentially all of the transmitted particles. By this means we could determine the double differential transmission function $d^2T/d\Omega dE$ as a function of incident energy and compare it with the large-solid-angle detector yield (the integrated transmission $T(E_{inc})$). The primary beam energy was stepped over an energy interval which included the proton energy corresponding to the appropriate range in beryllium (0.25 mm or 1.75 mm).

The range determined by the 50% point in the transmission curve T(E) was found to be in good agreement with the range tables of Williamson.[1] Using the large-solid-angle detector spectrum dY/dE extrapolated to zero energy we determined a transmission/keV interval at zero energy of about $10^{-4}$, consistent with crude estimates based on straggling considerations, and to be compared with a value $3\times10^{-5}$ obtained by more precise time-of-flight methods described below (see Sec. 6.3). This transmission fraction is a factor in determining how many trappable particles survive the energy loss process. A value much lower than $10^{-5}$ would make this trapping method impractical.

The most surprising result of this project was the observation in the $d^2T/d\Omega dE$ data of an apparent high correlation between energy loss and multiple scattering angle. This correlation is such that the particles suffering the largest energy loss also are scattered furthest away from the the incident beam direction. The average deviation angle (not the rms angle) was about 5° for instance for the 5 MeV incident beam. Because of this correlation the number of lowest energy particles scattered back into the incident beam direction is greatly reduced from what one would expect if there were not a strong correlation. Thus, when the incident beam is nearly ranged out in the degrader foil the lowest energy particles to emerge seem to form a hollow cone. This result has required for the antiproton trapping experiment that a

36

large fraction of the energy degrader material be placed as close as possible to the trap, to increase solid angle and to restrict radial motion of the ions with the 6T magnetic field surrounding the trap.

References:

*   Department of Physics, University of Washington.
1.  C. Williamson and J.P. Boujot, Rapport CEA No. 2189 (1962).

## 6.3   Observation by Time-of-Flight Methods of 1 keV Protons and Antiprotons Slowed from 16 and 21 MeV in Beryllium

X. Fei,[*]   G. Gabrielse,[*]   K. Helmerson,[*]   S. Rolston,[*]   R. Tjoelker,[*]   and T.A. Trainor[*]

As part of our program to measure the mass of the antiproton in a Penning trap it is required to demonstrate that a significant number of antiprotons can be slowed from 21 MeV (the lowest energy presently avaliable at LEAR) to about 1 keV where, in principle, particles within a certain solid angle can be trapped. The particles are slowed in a beryllium degrader foil.

To determine the yield near 1 keV we have developed a time-of-flight system consisting of a 0.13 mm thick plastic (polystyrene) scintillator and a channel plate detector. The particle beam passes from vacuum to air through a 0.13 mm beryllium window, passes through the thin plastic detector, and returns to vacuum through an identical beryllium window. The second vacuum system contains a thick beryllium degrader followed by a channel plate detector. The degrader and channel plate front surface are separated by a 26 mm flight path.

Signals from the plastic detector phototube and channel plate preamplifier each pass through one stage of fast amplification and enter Ortec 473 constant fraction discriminators. Discriminator signals then pass to an Ortec 437A time-to-amplitude converter with the plastic detector used as the stop. The TAC output is digitized and stored in computer memory as a time spectrum histogram by standard techniques. This is essentially the spectrum of times of flight for particles emerging from the beryllium foil and travelling 26 mm to the channel plate. The plastic detector is observed to be 100% efficient at the incident particle energy (demonstrated for protons, inferred for antiprotons), and the channel plate is observed to be >80% efficient for energies above 100 keV. We have no evidence that the channel plate is not 100% efficient down to several keV particle energy.

To understand the structure of the time spectrum it is convenient to consider a simplified energy spectrum with uniform density from zero up to some maximum energy $E_o$. In fact, for spectra of nearly stopped particles this is a useful approximation. The corresponding time spectrum is a $1/t^3$ distribution starting at minimum time $t_o$ (flight time of particles with $E=E_o$) and falling away as $t$ increases. For the flight path indicated 1 keV particles have a transit time of nearly 60 ns. For times larger that $t_o$ there

is a random background determined largely by the plastic detector rate (maintained at 1-5 kHz for optimum signal/noise). For times smaller than $t_o$ the random background is determined by the dark count rate in the channel plate and is not important in this case.

In practice a region of the time spectrum is integrated which corresponds to a range of particle energies near 1 keV (say 30-60 ns) and the random background contribution subtracted away. This net yield, divided by the corresponding energy range in keV is a critical parameter for determining feasibility of the antiproton trapping scheme.

This system was developed with a 16 MeV proton beam at the NPL. The beam energy was varied over an interval within which the protons should come out in the selected beryllium degrader. The yield/keV was determined above and the transmission (channel plate/plastic yield) were plotted as functions of energy. The half-maximum point in the transmission curve agreed well with the range table of Williamson.[1] And the maximum yield/keV at 1 keV was found to be $3\times10^{-3}$ relative to the incident beam flux.

The same apparatus was then carried to CERN (May, 1986) and installed on a beam line at the LEAR antiproton facility. In this case the beam has a fixed energy so the degrader thickness was varied in steps using a foil wheel. The range in beryllium determined for 21.3 MeV antiprotons (3.03 mm) agreed well (<2%) with the Williamson table for protons, and the yield/keV at about 1 keV was determined to be greater than $10^{-3}$/keV, and not significantly different from the proton number.

These results indicate that brute-force slowing of antiprotons in a degrader produces a sufficient flux of particles at 1 keV to make trapping feasible, other things being equal, and that the slowing process in beryllium seems to be the same for antiprotons as for protons, at least down to 1 keV.

References:

*    Department of Physics, University of Washington.
1.   C. Williamson and J.P. Boujot, Rapport CEA No. 2189 (1962).

******

## 6.4   Alignment and Installation of the H-Atom Solenoid

T.A Trainor and P. Wong

Since the last Annual Report we have trimmed the solenoid by inserting shims between the individual coils to investigate the feasibility of reducing transverse fields in this manner. The scanning procedure discussed previously[1], was used to verify the B-field homogeneity. We have reduced variations in the transverse directions $(B_x, B_y)$ to a few parts in $10^5$ of the field in the axial direction $(B_z)$.

Having achieved this field quality we decided to operate without a flux return since the iron would introduce hysteresis (causing asymmetric B-field reversal) and would complicate the shimming procedure by perturbing the field. The field could be retrimmed only by removing the flux return (which prevents access to the shims), making the required adjustments, replacing the flux return and remeasuring the field. Many attempts would be required before the field could be straightened. With the addition of a third power supply and proper shunt arrangement a uniform field can be produced in the region of the RF cavities without an iron flux return.

Several months were spent redesigning a system to support the new solenoid and replacing iron components in the apparatus which could affect the unshielded magnetic field. After removing or replacing the major sources of field perturbation, the solenoid was installed in the apparatus (on temporary support jigs during the completion of the final version) and a series of field scans were made to locate any source of field disturbance. The only problem preventing symmetric field reversal were the ion pump and the iron end-plate welded to one end of the ultrahigh vacuum vessel. Fortunately, the pump's effect does not extend into the region of the RF cavities, and the effect of the iron end-plate depends on the existence of an external non-reversing field (in this case the earth's field). This problem will be removed by adding Helmholts coils to null the earth's field.

The solenoid was retrimmed and the shunts controlling the homogeneity of axial field were adjusted. The field produced is uniform to $\pm 5 \times 10^{-5}$ over 80% of the RF cavity region in all three axes, and reaches a maximum error of $10^{-4}$ in the transverse directions, and a maximum error of $4 \times 10^{-4}$ in the axial direction. The worst case errors are all located at the upstream end of the RF region, well away from the sensitive "long" cavity. This performance is more than a factor of 10 better than achieved by the old copper-wound solenoid. It is hoped that this improvement will enable us to identify and remove the source of stray electric fields in the RF cavity and lead to an eventual improvement in the sensitivity for detecting parity violating amplitudes by one or two orders of magnitude.

Reference:

1.  Nuclear Physics Laboratory Annual Report, University of Washington, (1985) p. 42.

39

7. MEDIUM ENERGY PHYSICS

7.1 Direct-Semidirect Calculation for the $(\gamma, n)$ Reaction

P.T. Debevec,[*] D.H. Dowell,[†] I. Halpern, L.J. Morford,[*] T. Murakami,
D.W. Storm, and S.A. Wender[‡]

Last year we found that the fore-aft asymmetry in the $(\gamma, n)$ reaction to the lowest levels in Pb increases from about 0.2 to 0.8 between 20 and 30 MeV.[1] Cd behaves similarly at somewhat higher photon energy. We have been studying these asymmetries and some related cross-sections in an attempt to extract from them the values of the parameters which characterize the E2 isovector giant resonance.

To determine the E2 parameter values we have used the direct/semi-direct model.[2] The observed asymmetry is found to depend only weakly on the magnitudes of the interfering odd-and-even parity amplitudes but strongly on their relative phases. Although most of this phase difference arises from the resonant character of the E2 amplitude in the excitation energy region under study, there are a number of other factors which contribute.

Unfortunately some of these factors are not very well pinned down. The factors include (i) the dependence of the E1 phase on the ratio of the direct to the resonant E1 amplitude, (ii) the difference in phase shifts for out-going neutrons which arise from the optical potential acting on particles of differing orbital angular momentum. (For any particular single-hole state, the outgoing neutrons will have differing angular momenta for excitations of different parity) and, (iii) the complex particle–vibration coupling constants in the numerators of the resonant amplitudes.

Despite the reservations associated with the phase uncertainties from these factors, the center of the E2 isovector resonance in Pb is found to be located at 23.5 MeV within ±1.5 MeV.[3] The resonance appears to be about 6 MeV wide, but this width and the estimated resonance strength remain somewhat uncertain.

References:

\* University of Illinois, Urbana, IL 61801.
† Brookhaven National Laboratory, Upton, NY 11973.
‡ Los Alamos National Laboratory, Los Alamos, NM 87545.
1. Nuclear Physics Laboratory Annual Report, University of Washington (1984) p. 16.
2. Nuclear Physics Laboratory Annual Report, University of Washington (1985) p. 23.
3. T. Murakami, I. Halpern, D.W. Storm, P.T. Debevec, L.J. Morford, S.A. Wender, and D.H. Dowell (to be published).

\*\*\*\*\*\*

7.2   **Forward-to-Backward Asymmetry in the (γ,n) Reaction in the Energy Range of 28-39 MeV**

D. Dale,[*] P.T. Debevec,[*] A. Freytag,[*] C.A. Gossett, I. Halpern, R. McCrady, T. Murakami, D.P. Rosenzweig, D.W. Storm, and D.R. Tieger

Continuing our systematic survey of the E2 isovector resonance in nuclei, we measured the fore-aft asymmetries in the (γ,n) reaction for $^{nat}$Ca and Pb at energies between 28 and 39 MeV. As described in Sec. 7.1 and in last year's report,[1] these asymmetries arise from the interference of the E2 isovector resonance centered at $E_{x} \approx 130A^{-1/3}$ in heavy nuclei with odd parity excitations at the same energies. The main motivations in this year's run were to see whether the E2 resonance shifted monotonically to higher energies as the A of the target was reduced and to see what happens to the asymmetry at energies well above resonance. The latter point was investigated with the Pb target.

The experiment was performed using the continuous electron beam of the University of Illinois MUSL-2 electron microtron, at an energy of 49.2 MeV, along with their photon-tagging facility. Neutrons were detected in three newly fabricated NE-213 liquid scintillators which were 30 cm in diameter and 10 cm thick. Data were recorded event by event on magnetic tape using a new data-acquisition system.

The data are currently being analyzed. Very preliminary results show asymmetries in Ca which rise steadily from ≈0.10 at 28 MeV to levels of 0.4 to 0.6 between 34 and 39 MeV. This behavior is in reasonable accord with what one might expect from the Ca (γ,n) results of Bergqvist et al.[2] The asymmetry for Pb goes through a flat peak at ~ 28 MeV.

**References**

*   University of Illinois, Urbana, IL 61801.

1.  Nuclear Physics Laboratory Annual Report, University of Washington (1985) p. 23.

2.  I. Bergqvist et al., 419, 509 (1984).

\* \* \* \* \* \*

41

7.3    Inclusive Scattering of Pions from very Light Nuclei at 100 MeV

J.F. Amann,[*] W.J. Burger,[†] K.G.R. Doss,[+] D.H. Dowell,[x] I. Halpern,
M.A. Khandaker, D.D. Leach, T. Murakami, D.W. Storm, and D.R. Tieger

In continuing our effort to study the pion-nucleon interaction in the
nuclear medium we have measured the inclusive energy spectra and angular
distributions of 100 MeV pions inelastically scattered from $^4$H and $^{3,4}$He. One
important aim of this study is to learn about the effects of pion attenuation
and absorption through their effects on the scattering process.

Details of the experimental procedures and results have been reported in
earlier annual reports[1]. The angular distributions in the backward hemisphere
($\theta_{lab} > 75^\circ$) for all three nuclei closely resemble that of scattering from a
free proton. This is interpreted to indicate the quasi-elastic nature of these
backward scatterings. The relative $\pi^-$ cross-sections (integrated over angles
and outgoing pion energies and normalized to $^1$H) are $0.69 \pm 0.02$, $1.42 \pm 0.04$ and
$0.88 \pm 0.02$ for $^2$H, $^3$He and $^4$He respectively. The corresponding $\pi^-$ cross-
sections for $^3$He and $^4$He are $0.68 \pm 0.03$ and $0.90 \pm 0.03$. It is seen that the
relative cross-sections here have been measured to about $\pm 5\%$.

Based on the success of the quasi-elastic scattering picture in
accounting for the backward inelastic scattering of pions from heavy nuclei[2]
we have carried out plane and distorted wave impulse approximation
calculations to see how well they could account for the observed spectral
shapes and cross-section ratios.

Even the plane wave calculations are found to reproduce the spectra very
well, except that they (understandably) miss the enhancements in $^4$He due to
its low lying unbound resonances. We have not yet included the effects of pion
absorption into our calculations. However it seems unlikely that we will be
able to fully exploit the high precision of the measured cross-section ratios
to constrain the assumed parameters for the absorption process. The limitation
seems to be the uncertainty in the relative normalizations of the impulse
approximation cross-sections for our three targets.

References:

*   Los Alamos National Laboratory (LAMPF), Los Alamos, NM 87545.
†   Massachusetts Institute of Technology, Cambridge, MA 02139.
+   Lawrence Berkeley Laboratory, Berkeley, CA 94720.
x   Brookhaven National Laboratory, Upton, NY 11973.
1.  Nuclear Physics Laboratory Annual Report, University of Washington (1984)
    p. 52 and ibid. (1985) p. 48.
2.  K. Aniol et al., Phys. Rev. C 33, 208 (1986).

8. ACCELERATOR MASS SPECTROMETRY (AMS)*

D.R. Balsley, G.W. Farwell, P.M. Grootes,[†] D.D. Leach, and F.H. Schmidt

8.1 AMS: Scientific Program

Measurements of $^{14}C/^{12/13}C$ isotopic fractions in the range of $10^{-12}$ to $10^{-15}$ have been continued. We are able to measure the $^{14}C$ content of modern carbon samples from environmental materials with accuracy in the range of 1% to 1.5%, based upon two or more measurements each lasting up to one hour. The results of the study of thin sections of annual tree rings in Sitka spruce,[1,2] which demonstrate the rapid response of wood cellulose to changes in atmospheric $^{14}CO_2$ concentration, have been submitted for publication. We have also completed our collaborative work on dissolved and particulate organic carbon in the Amazon River System (different fractions exhibit different apparent residence times), and the results have been published.[1,3,4] Other radiocarbon studies undertaken include the following:

A. Algae samples from lakes in the dry valleys of Antarctica were dated in order to assist in the reconstruction of the climatic history of Antarctica.[4]

B. Results were obtained on the organic $^{14}C$ concentrations in deep-sea surface sediments from locations in the Equatorial Pacific, the continental slope of the northeastern United States, and off the southern California borderlands; surprisingly, variations are seen within the bioturbated layer (the top few cm) of the sediments. Modeling studies and further measurements are being undertaken.[3]

C. Our prospects for the measurement of very old $^{14}C$-containing samples have been further improved by the establishment of a background (equivalent age) of about 60,000 years for the AMS system and of about 50,000 years for a prepared sample containing 5 mg of carbon.*

D. We have begun a collaboration with colleagues in the School of Oceanography (D.D. Quay and others), supported in part by a NASA grant, on an integrated isotopic investigation of methane cycling in a high northern-latitude wetland environment (Alaskan tundra).

References:

* Our work has been supported in part by the National Science Foundation (Grant EAR-8115994, Environmental Geosciences Program).

† Quaternary Isotope Laboratory and Departments of Geological Sciences and of Physics, University of Washington.

1. Nuclear Physics Laboratory Annual Report, University of Washington (1985) p. 51.

2. P.M. Grootes, M. Stuiver, G.W. Farwell, D.D. Leach, and F.H. Schmidt, 12th International Radiocarbon Conference, Trondheim, Norway, June, 1985 (abstract).

3. J.I. Hedges, J.R. Ertel, P.D. Quay, P.M. Grootes, J.E. Richey, A.H. Devol,

G.W. Farwell, F.H. Schmidt, and E. Salati, Science 231, 1129 (1986).
4. P.M. Grootes, M. Stuiver, G.W. Farwell, D.D. Leach, and F.H. Schmidt, Radiocarbon (in press).
5. S.R. Emerson, C. Stump, P.M. Grootes, M. Stuiver, G.W. Farwell, and F.H. Schmidt, American Geophysical Union, Ocean Sciences Meeting, January 13-17, 1986 (abstract).

****** 

## 8.2 AMS: Technical Improvements

### A. Sputter Ion Source

An extensive modification program has been successfully completed; the source now produces twice as much useful beam as previously, viz., 25-30 $\mu A$ $^{12}C$ ions. Details are given elsewhere in this report (see Sec. 11.3).

### B. Normalization

We have made a number of important improvements in our two systems of normalization of $^{14}C$ counts, viz., to $^{13}C$ and to $^{12}C$, and the entire system is now programmed to operate automatically. We can now choose data timing sequences to match the demands for different sample activities; for example, we can alternate long with short counting times.

### C. Ion Optics and Transmission

We have studied the ion optics and transmission of the entire AMS system. These studies have resulted in a number of improvements, the most important of which are enumerated below.

1) The 24-inch chamber beam-line magnetic quadrupole was moved upstream to reduce the partial interception of beam that occurs under unfavorable conditions in the tandem.

2) The velocity selector has been doubled in length so as to double the effective velocity dispersion. The result is a cleaner spectrum in the final detector telescope. In addition, the use of a larger vertical detector aperture is permitted, so that the overall $^{14}C$ transmission is more stable.

3) We have devised a beam alignment procedure which largely circumvents aberrations found in the double-focussing 90° main analyzing magnet.

Two innovations in the $^{12}C$ normalization procedure appear promising. First, a change in the shape of the entrance aperture for the low-energy auxiliary faraday cup has improved the agreement between results by $^{12}C$ and $^{13}C$ normalizations. Second, a sequential mode of alternation between standard and unknown samples has been introduced that has the potential for improving the rate at which we can make a series of measurements.

9.    NUCLEAR STRUCTURE

9.1   Low Energy Resonances in $^{13}$N Studied Via $^{12}$C($\vec{p}$,p)

E.G. Adelberger, C.A. Gossett, J. Sromicki,[*] and V.J. Zeps

We have chosen to exploit resonances observed in proton elastic scattering from $^{12}$C to test for false asymmetries in our experiment to measure the parity mixing in $^{14}$N (See Sec. 4.4). The $^{13}$N system has two low lying overlapping resonances, $J^{\pi}=3/2$ and $5/2$ at $E_x = 1.69$ and $1.73$ MeV, respectively, which produce large transverse analyzing powers in the detectors of the $^{14}$N experiment. The large transverse analyzing powers in $^{12}$C+p compared to those in $^{14}$N give greatly increased sensitivity to the spin dependent systematic effects which produce false longitudinal asymmetries.

During an experiment to measure the low energy structure in $^{14}$N from $^{12}$C($\vec{p}$,p) (see Ref. 1) we also studied proton elastic scattering from $^{12}$C in order to correct for carbon buildup on the target. The cross section and analyzing powers for $^{12}$C($\vec{p}$,p) for $E_x=1.0$ to $3.4$ MeV were measured using eight solid state detectors at center of mass angles 39.4, 55.3, 70.9, 91.3, 124.2, 138.4, 152.4, and 166.3°. The absolute solid angle normalization was obtained from proton elastic scattering from a gold target. During the past year an R matrix description for the cross section and analyzing power for proton scattering from spin zero targets has been independently derived following the formalism of Lane and Thomas[2]. A computer code incorporating a least squares fitting procedure with the R matrix description has been written. Our preliminary results indicate that the resonance parameters of Ref. 3 do not describe the structure observed in our experiment. In particular our analysis suggests widths for the $3/2$ and $5/2$ resonances which are substantially smaller than those of Ref. 3 and are in much better agreement with the R matrix analysis of Ref. 4. A complete analysis is in progress.

References:

*   Department of Physics, University of Wisconsin, Madison, WI 53706.
1.  Nuclear Physics Laboratory Annual Report, University of Washington (1985) p. 6.
2.  A.M. Lane and R.G. Thomas, Rev. Mod. Phys. 30, 257 (1958).
3.  F. Ajzenberg-Selove, Nucl. Phys. A 360, 1 (1981).
4.  H.O. Meyer, G.R. Plattner, and I. Sick, Z. Phys. A279, 41 (1976).
5.  Nuclear Physics Laboratory Annual Report, University of Washington (1984) p. 44.
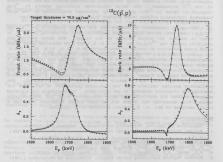
Fig. 9.1 — The points are countrate and analyzing power measurements for $^{12}C(\vec{p},p)$ using the $^{14}N$ parity experiment chamber.[5] The curves are predictions from the R-matrix calculation, where an integration over target thickness and detector angle has been performed. The target thickness was chosen to match the rates, and polarization was varied to match the analyzing powers.

## 9.2  β-Forbidden Beta Decay of $^{207}$Tl

E.G. Adelberger, M.M. Hindi, S.E. Kellogg, and T. Murakami

The $1/2^--5/2^-$ β decay of $^{207}$Tl to the 570-keV first excited state of $^{207}$Pb is a unique first-forbidden decay. The $^{207}$Tl ground state is, to first order, a 3s$_{1/2}$ proton hole and the $^{207}$Pb 570-keV state is a 2f$_{5/2}$ neutron hole. Thus the orbital angular momentum change involved in the decay is Δℓ=3. The first-forbidden decay operator, however, can change the orbital angular momentum by one unit; therefore to first order this decay is ℓ-forbidden. Hence the dominant contributions to the decay are expected to come from core polarization, Δ-N$^{-1}$ admixtures and exchange currents. To assess the importance of such terms we have searched for the decay $^{207}$Tl(βγ$_1$)$^{207}$Pb.

The $^{207}$Tl activity was produced by depositing 0.5 mC of $^{211}$Ra onto a cation exchange column and eluting the $^{207}$Tl activity with 0.5 N HCl. Gammas were counted in a 45 cc Ge(Li) surrounded by a NaI shield consisting of an annular detector 30.0 cm long × 21.5 cm outer diameter with an 8.9 cm inner diameter, and 7.6 cm × 7.6 cm NaI detector to close one end of the annulus. The NaI array served as an anti-compton shield as well as an anti-coincidence suppressor for the 328-keV γ-ray which results when the 570-keV state is fed by the decay of the 898-keV second excited state in $^{207}$Pb.

The 328-keV, 570-keV and 898-keV γ-rays from the $^{207}$Tl decay were observed as well as γ-rays from the $^{211}$Bi and $^{207}$Pb parents, and from $^{214}$Pb, $^{214}$Bi and $^{228}$Th which result from $^{226}$Ra and $^{228}$Th contaminants in the $^{211}$Ra source.

The γ-ray intensity of the 328-keV line relative to the 898-keV line was found to be (0.57±0.04)%, in agreement with the less precise value (0.64±0.2)% found in Ref. 1. After correcting for the indirect feedings $^{211}$Bi(β)$^{207}$Po(α)$^{207}$Pb(570) and $^{207}$Tl(β)$^{207}$Pb(898)(γ$_{z,1}$)$^{207}$Pb(570) we find a beta branch of $^{207}$Tl to the 570-keV level, relative to the branch to the 898-keV level of <4×10$^{-4}$. Using the value (0.24±0.04)% for the latter branch, our result then translates to an intensity of <1×10$^{-6}$ per $^{207}$Tl decay. This limit is two orders of magnitude lower than the previously established limit.

### References:

1.  L.J. Jardine, Phys. Rev. C 11, 1385 (1975).

2.  W.F. Davidson, C.R. Cothern, and R.D. Connor, Can. J. Phys. 45, 2295 (1967).

10.    RESEARCH BY OUTSIDE USERS

10.1   Measurement of Total Body Calcium by Neutron Activation

C.H. Chesnut,[*] B.L. Lewellen,[*] and R. Murano[*]

We have now completed 16 years using neutron activation at the 60"
cyclotron to measure total body calcium in patients with bone wasting
disease.[*] The total body calcium by neutron activation analysis determination
has proven to be a precise and accurate quantitation of total body bone mass
(total skeletal calcium), and indeed is the "gold standard" by which other
developing bone mass measuring techniques are measured. The TBC technique has
been utilized in our lab in assessing response to therapy with anabolic
steroids (methandrostenolone and stanozolol), synthetic salmon calcitonin, the
active form of Vitamin D (calcitriol), and a number of diphosphonate
compounds. Newly developed technique for quantitating bone mass, including
dual photon absorptiometry at the spine and hip, computerized axial tomography
of the spine, single photon absorptiometry at the wrist, and ultrasound
measurements at the knee, are compared to the total body calcium technique to
determine their overall efficacy.

In the past year we performed 165 patient irradiations. Two therapeutic
regimes were under test. Under the first regime, patients were treated with
1.25 dihydroxy calciferol (Vitamin D).[2] Under the second regime, patients were
treated with a sequential dosage of phosphate and Didronel[3] and were followed
after withdrawal of the drug. In both studies, an equal number of untreated
control subjects were followed and many other tests were performed as well as
neutron activation. Since June, 1982 we have also been measuring the bone
mineral in the lumbar spine by the dual photon absorption technique developed
by Mazess of the University of Wisconsin and applied extensively by Wahner et
al.[*] of the Mayo Clinic, and comparing it to the total body calcium - neutron
activation analyses technique.

References:

*    Division of Nuclear Medicine, University of Washington.
1.   Nuclear Physics Laboratory Annual Reports, University of Washington (1967-
     1982).
2.   Hoffman-LaRoche Laboratories.
3.   Proctor and Gamble.
4.   H.W. Wahner, W.L. Dunn, R.B. Mazess, M. Towsley, R. Lindsay, L. Markhard,
     and B. Dempster, Radiology 156, 203 (1985).

******

## 10.2 Irradiation of Optical Materials

T.L. Criswell[*],    K.L. Ballou[*],    G. Bohnhoff-Hlavacek[*],    and    V.S. Starkovich

Reflection of light from transparencies (e.g., the inside of windshields, CRT screens, or instrument covers) is a chronic problem. Existing antireflective coatings, while reducing reflection, often work in too narrow band of frequencies, are absorptive, or produce excessive diffuse scattering. The fundamental cause of reflection is the abrupt change in the index of refraction at the interface between the two media, air and the transparency. If the change in the index can be smoothed over distances of the order of the wavelength of light, the reflectivity will be reduced. Such smoothing can be achieved by producing a dendritic surface with an areal-average index. A method of producing such surfaces has been developed by adapting techniques used in nuclear track-etch detectors. Dielectric materials are irradiated with high fluences of heavy ions and the resulting damage tracks are chemically etched away. The remaining walls of the etch pits approximate the desired shape. The exact shape of the pit wall depends on the damage threshold of the material, the stopping power of the ion, and the etch process. The present study covers a wide selection of plastics and glasses, finding optimum ion-etch combinations to produce the desired antireflective surface for each material. Over 1200 samples were tested this year using seven ions and as many as three energies per ion. Results to date have been quite good. Samples have been produced with specular reflectivity reduced by more than three orders of magnitude. Plans are being made to develop a large-sample (1m × 1m) irradiation facility to test the process at the component level.

### Reference:

* Boeing Aerospace Company, Seattle, WA  98124-2499.

******

## 10.3 Irradiation of GaAs Solar Cells

D.A. Russell[*] and S.A. Billets[†]

Proton irradiations were performed on Metal-Organic Chemical Vapor Deposition (MOCVD) type GaAs solar cells using the Van de Graaff accelerator. The purpose of the 3, 6, and 10 MeV irradiations was to study the solar cell degradation associated with a space environment and with selected cell design variables.

### References:

* Boeing Aerospace Company, Seattle, WA  98124-2499.
† Lockheed Missiles and Space Co., Sunnyvale, CA  94086.

###### ******

## 10.4 Experiments Supporting Accelerator Development at the Boeing Company

T.D. Hayward,[*] A. Berron Jr.,[*] and D.A. Russell[*]

The Boeing Aerospace Company is investigating development of a linear accelerator for $^3$He ions with energies of about 20 MeV.

Measurements were made of the stripping of $^3$He$^-$ ions induced by an electric field. This is of interest because an electron is very weakly bound to $^3$He and can be stripped in the strong electric fields in a linear accelerator. It was found that the threshold for electric field stripping was 17 MV/m. It is concluded that a drift tube linear accelerator could be designed to accelerate $^3$He ions without losses due to electric field stripping.

Measurements were also made of the radiation environment around a tantalum beam stop when bombarded by $^3$He$^-$ ions. Measurements of the neutron dose were made using a Bonner-type detector for ion energies between 18 and 23 MeV. The dose increased approximately exponentially with energy. At 18 MeV it was about 2 mrem/hr at a distance of 1.35 meters for a beam current of 350 nA. It increased by an order of magnitude for every 3.4 MeV of ion energy. It is concluded that a $^3$He linear accelerator can be operated at energies near 20 MeV without large amounts of neutron shielding.

### Reference:

* Boeing Aerospace Company, Seattle, WA 98124-2499.

## 11. ACCELERATORS AND ION SOURCES

### 11.1 Van de Graaff Accelerator Operations and Development

D.R. Balsley, J.R. Cromie, D.J. Hodgkins, C.E. Linder, F.H. Schmidt,
R.E. Stowell, T.D. Van Wechel and W.G. Weitkamp

To better accommodate the personnel and time requirements of the booster installation, operation of the tandem accelerator was reduced by 1/3 beginning in March 1986. All maintenance and development has been held to the minimum required to support the attenuated research schedule.

In August the injector tandem was dismantled and shipped to Lawrence Livermore Laboratory where it will be installed as a replacement for an older tandem accelerator. The hole where the injector had been was covered over by concrete slabs which can be moved to give access to the pit under the tandem.

Because of fortuitous circumstances, the old Lamb-shift polarized hydrogen ion source proved to be an excellent source of negative helium ions. When the Lamb-shift source was taken off the accelerator to make room for the new polarized source, we removed those parts needed to build a stand-alone helium ion source. This project is described in Sec. 11.4. The new polarized ion source project is described in Sec. 11.5

The sputter source continues to be upgraded. This is described in Sec. 11.3.

The radiation safety system around the tandem is growing unreliable due to the age of the instruments. We are updating the radiation monitors and will hook the system up to the programmable controller which will oversee radiation safety in the booster area, described in Sec. 14.3.

Problems with poor transmission through the machine were traced to possible intermittent shorts across the insulators in the low energy electrostatic quadrupole lens. To eliminate that possibility, the lens was rebuilt using Macor slabs to support the electrodes. The lens now holds up to 10 kV reliably.

During the year from April 16, 1985 to April 15, 1986 the tandem operated 3705 hours. Additional statistics of accelerator operations are given in Table 11.1.

Table 11.1
Tandem Accelerator Operations
April 16, 1985 to April 15, 1986

| Activity | Days Scheduled | Percent |
|---|---|---|
| A. Nuclear Physics Research | | |
| Light Ions | 79 | 22 |
| Heavy Ions | 67 | 18 |
| Radiochronology | 47 | 13 |
| Total | 193 | 53 |
| B. Outside Users | | |
| The Boeing Company | 5 | 1 |
| Lockheed | 2 | 1 |
| Total | 7 | 2 |
| C. Other Operations | | |
| Accelerator Development | 74 | 20 |
| Accelerator Maintenance | 38 | 10 |
| Unscheduled Time | 53 | 15 |
| Total | 165 | 45 |
| Grand Total | 365 | 100 |

******

## 11.2 Cyclotron Operations and Development

J.R. Cromie, H. Fauska, B.L. Lewellen,[*] R. Murano,[*] R.E. Stowell, and
W.G. Weitkamp

Now in its 34th year of operation, the 60 in. cyclotron is used almost
exclusively for the in vivo calcium measurements conducted by the Division of
Nuclear Medicine, described in Sec. 10.1. The aging vacuum seals continue to
provide most of the maintenance problems; rubber gaskets have succumbed to
radiation or chemical damage and metal surfaces have become corroded or
galled, making repair difficult.

The machine ran 247 hours between April 16, 1985 and April 15, 1986. It
was scheduled for 91 days. Approximately 13 days were lost to operations
because of maintenance problems.

Reference:

* Nuclear Medicine, University of Washington.

## 11.3 Sputter Ion Source Improvements

### D.R. Balsley, D.J. Hodgkins, and F.H. Schmidt

In May, 1985, the source was modified to include a four-sectored Einzel lens to focus and steer the Cs beam. Initial tests gave improved outputs: 10 μA $^{12}$C at the LE Cup from a graphite sample, but were limited by inverse loading of the Cs focusing and steering supplies by secondary electrons. The inverse loading problem was relieved by increasing the load of the bias resistors on the Cs focus supply to absorb secondaries, and by building a new regulated steering supply.

A higher reflection voltage was tried in August, running at six to eight kV rather than 200-300 volts. This higher mode gave a somewhat higher beam current at high outputs, and most importantly it produced a sharper focus of Cs on the sample face, and a correspondingly sharper beam. There is some evidence that the "low mode" may be better at low output levels, but this has not been thoroughly explored.

As the above improvements allowed beam output to be increased by raising the sputter wheel or "extraction" current, above the previous limit of 1 mA, concern grew about the large loading of the elevation supply from secondary electrons. A magnetic suppression system was designed and installed around the bellows just downstream from the source, which dropped the elevation current by a factor of two, and decreased radiation at the source beamline valve by a factor of six.

There have been two different reflection/extraction geometries in use: the "nozzle" geometry, referring to operation with an aluminum insert which fits into the original accelerator electrode,[1] and the "standard" geometry, which is operation without the insert. At 30 kV elevation, the nozzle geometry gives a larger beam at the LE Cup than the standard geometry, apparently due to better transmission through the injection magnet. If the elevation is raised to 60 kV, however, beam from the two geometries is equivalent. The standard geometry has the advantages of sharper focus on the sample, a lower elevation current, and less trouble with sparking and accumulation of dirt. With the current LE Quadrupole Triplet power supplies the elevation is limited to 30 kV, so the nozzle geometry is being maintained, with a new stainless steel insert replacing the aluminum.

Since January of 1986, runs incorporating all of the above improvements have resulted in record performance. The source is now operated routinely at extraction currents above 1.5 mA and as high as 3.0 mA, with a new laboratory record output of 70 μA $^{12}$C from a graphite sample.

### Reference:

1. Nuclear Physics Laboratory Annual Report, University of Washington (1981) p. 177.

## 11.4 Modification of Alpha Source

D.R. Balsley, D.J. Hodgkins, and W.G. Weitkamp

The cesium box of the old Lamb-shift Polarized Ion Source has been used as a source of unpolarized $^3$He and $^4$He beams for some time. In November, 1985, the old Polarized Ion Source was dismantled to make room for the new crossed-beams source. The new source will not have the capacity to produce He beams, so the cesium box of the old PIS was modified to be interchangeable with the Sputter Ion Source on an elevated frame previously used only for the sputter source. The cesium box (generally referred to as the alpha source) consists of a duoplasmatron and a heated canal filled with cesium vapor. Positive helium ions extracted from the duoplasmatron pass through the canal, collide with neutral cesium atoms, and emerge as negative helium.

In order to accommodate the power supplies for the alpha source, the elevated platform and surrounding fence were enlarged so that a new rack could be located next to the current rack of SpIS supplies. The power lines to the new rack were wired using the existing interlocks of the SpIS system, and a switch was installed on the source frame so that only one rack can receive power at any time. In addition, the three-phase isolation transformer from the old source was installed in the new rack to bring power to the duoplasmatron supplies, which are elevated to 3500 V.

The high-voltage leads from the supplies in both racks are brought across a cable tray to the source frame where they plug into one side of an insulated patch panel below the source stand. Short cables coming from the source in use can then be plugged into the appropriate sockets on the other side of the patch panel. This way high voltage lines are easy to switch, and safe from accidental contact.

A freon pump was installed in the pit beneath the tandem to provide cooling for the duoplasmatron and for a new cesium trap in the alpha source. The cesium trap is located just downstream of the cesium canal, and is designed to minimize the amount of cesium drifting into the pump tee and acceleration tube. In its initial operation it appears to work very well.

The physical support and alignment structure of the alpha source was modified to be compatible with the existing SpIS support plate. The alignment systems for the two sources are entirely independent, so there is no significant re-alignment necessary when switching from one source to the other.

In its first run, April 1986, the source gave a $^3$He beam of 200-800 nA at the 1Z cup, and several μA of un-analyzed beam at the source Faraday cup upstream of magnet #2. As the new system is better understood and stabilized, source performance and transmission through the magnet should improve.

******

54

## 11.5  Polarized Ion Source

D. Badt, J.G. Douglas, R. Hobbs, J.R. Olson, and T.A. Trainor

The last major assembly required for off-line operation of the crossed-beams polarized source, the calorimeter and rf transition region, was completed in October, 1985.  Following a period of development the source produced 700 nA of polarized H$^-$ at 40 keV through the spin precessor in February, 1986.  The neutral cesium beam flux through the ionizer was ≈7mA.  We then moved the source to its permanent site in the accelerator ion source area.  During the move we redesigned and constructed replacements for a number of items in the neutralizer region which were observed to have short life times or inappropriate operation during the initial development period.

In late May, 1986, the source was returned to operation with cesium beam performance similar to what was observed before the move.  The improvements in the neutralizer region have led to much more stable operation.

We are now proceeding on a vigorous development program for the atomic beam source, whose output is observed, by pressure rise in a pumped volume, to be 10-20 times lower than expected.

55

## 12. NUCLEAR INSTRUMENTATION

### 12.1 Target Preparation

G.M. Hinn

In the table below are listed a few of the more interesting targets prepared in the Laboratory last year.

| Target | Starting Form | Final Form | Method of Preparation | Backing | Thickness in mg/cm |
|--------|---------------|------------|-----------------------|---------|---------------------|
| $^{148}Sm$ | oxide | metal | reduction evaporation | 10 µg C | 0.1 (strip) |
| $^{208}Pb$ | oxide | metal | $H_2$ reduction | S.S. | 1 |
| $^6Li_2O$ | metal | oxide | evaporation oxidation | S.S. | 1-2 |
| $^{nat}C$ | C powder | C strip | E-gun | 2µg C | 0.1 |
| $^{13}C$ | powder | C | E-gun | gold | 0.1 |
| $^{nat}Hf$ | metal | metal | E-gun | S.S. | 0.5 |

a. Stripper Foils. We have changed from using 3 µg/cm² cracked slacked foils to using collodion backed slacked 2 µg/cm² Arizona carbon foils. The new foils show better or equal transmission to that of the old foils.

b. Rolling Mill. We have acquired a two roller rolling mill from Freie Borel, 119 Third St., Oakland, CA 94604 as part of the target labs upgrading. We expect to use this mill for making heavy ion targets in the coming year.

c. Van Arkel de Boer Isotope Purification System. We are currently building an apparatus used in other labs (Oak Ridge and Garching, Germany) for purifying natural and enriched isotopes of hafnium, zirconium, and titanium. The method known commercially as "the hot wire process" developed by Van Arkel and de Boer in the 1930's uses a hot tungsten wire at 1600°C and crude (for example) hafnium to be purified at 600°C in a closed evacuated stainless steel container. Gaseous iodine is introduced into the container and it combines with hafnium to form hafnium iodide which sublimes at 400°C. When this hafnium iodide gas comes near the tungsten wire it decomposes leaving pure crystal bar hafnium metal on the wire. This is then rolled flat and the tungsten wire cut out.

### 12.1.1 Carbon Strip Targets Fabrication

G.M. Hinn, H.E. Swanson, and V.J. Zeps

Carbon strip targets were made using an apparatus which holds two razor blades' edges in close proximity forming a mask for a thin carbon strip deposited from the E-gun bombardment of natural high purity graphite rod. The strip was deposited onto a collodion backed 2 µg/cm² Arizona carbon foil. After deposition the foils, which were premounted on tantalum inserts, were placed in a tube furnace under vacuum and heated to 1000°C for 15 minutes. This evaporated off the collodion and relaxed the carbon foil and made it less fragile (See Sec. 4.3).

## 12.2 Design and Construction of Electronic Equipment

R.W. Abel,    H. Fauska,    J.M. Lacroix,    D.K. Morris,    D.B. Newell,
J.M. Stehfest, R.E. Stowell, and T.D. Van Wechel

Again this year, a majority of the electronics shop time was devoted to projects on the booster linac, described in Sec. 14 of this Annual Report. A list of the major projects follows.

a. A 1500 watt 150 MHz linear amplifier was constructed to allow conditioning of newly plated resonators for the linac.

b. A rather extensive controller for the linac vacuum system was designed and constructed, employing 160 outputs and 288 inputs.

c. Six more linac resonator controller chassis with associated power supplies were built for the linac satellite control stations. (see Sec. 14.10). A prototype was described and built last year.[1]

d. Forty additional rf control modules were constructed, utilizing modified Stony Brook controller boards described in last year's Annual Report.[1] Up to eight of these modules fit into the control chassis (descried in c. above) and allow independent control of phase and amplitude of individual resonators.

e. A magnet control chassis was designed and constructed to allow computer control of the linac dogleg Danfysik dipole magnets, the Bruker quadrupole magnets and the three 90 degree bending magnets.

f. An auxiliary electronics crate was designed and constructed to handle a variety of control and measurement functions at each satellite control station. This included cryogenic temperature control cards, analog bus cards, stepping motor cards (to run the couplers and tuners of resonators) and an isolating optical communications coupling link to the master control station in the control room.

g. An ion gauge controller simulator was designed and constructed for testing Ionvac controllers off-line.

h. The pretandem beam buncher constructed last year[1] was modified and tested to overcome severe internal heating and associated tuning problems (see Sec. 14.12).

When we were not working on booster projects, our major efforts were devoted to maintenance and repair of the general laboratory and Van de Graaff electronics and equipment.

Reference:

1. Nuclear Physics Laboratory Annual Report, University of Washington (1985) pp. 80-82, 83, 89.

## 12.3 Null Magnetometer with a Flux Gate Sensor

H. Fauska

To bring the beam from the tandem to the superconducting booster it was necessary to install a dipole magnet in the beam tube at the high energy end of the tandem. When the tandem is run without the booster, the residual magnetic field of this dipole must be degaussed. To sense the near-zero field remotely requires a stable and rugged sensor.

Since it is not necessary to know the flux in the dipole accurately but only that the flux is less than the earth's field, we designed a simple flux gate bridge[1] to sense the flux. The sensor is just two coils from reed relays epoxied together and one turn of magnetic ribbon taken from a ribbon-wound toroid threaded through the coils. It is important to keep the two coils electrically and magnetically equal. Therefore the ribbon should not overlap within either coil. The sensor is housed in an aluminum case sized to fit snugly in the magnet gap.

The driving electronics consists of two diodes driving a bridge containing the two coils and two bridge resistors. There is an additional balance potentiometer. The bridge is driven by capacitively coupled 400 Hz square waves.

A zero-center 50-0-50 microammeter connected between the resistor-to-coil junctions of the bridge gives local indication of the field. Remote readout requires a difference amplifier and an integrator. The integrator circuit changes the unidirectional pulses from the bridge into a direct current proportional to the differential change.

The instrument is a rugged remote sensor system with no moving parts.

### Reference:

1. W. Geyger, IEEE Trans. Comm., 68, Sept. 1963.

\*\*\*\*\*\*

## 12.4 Detection of Radionuclides from the Chernobyl Incident

S.E. Kellogg, J.H. Gundlach, and C.W. Stubbs

An air sampling system set up at the University of Washington Nuclear Physics Laboratory was able to detect airborne radionuclides emanating from the reactor incident at Chernobyl, USSR. The measurements were made during the month of May by drawing air through a filter and then taking a spectrum of gamma ray emissions from the filter with a Ge(Li) detector. Comparison with background spectra allowed unambiguous detection of $^{99}$Mo, $^{103}$Ru, $^{106}$Ru, $^{131}$I, $^{132}$Te, $^{132}$Te, $^{134}$Cs, $^{136}$Cs, $^{137}$Cs, $^{140}$Ba and $^{141}$Ce. These results are consistent with the isotopes observed in Europe, and we conclude that the Chernobyl event is the source of these shortlived airborne radioisotopes.

The filters used were "off the shelf" high quality commercial ventilation filters, Farr type 30/30, 95% efficient at trapping particles down to 5 microns, and 50% efficient at 2 microns. Air was drawn through the filters with a large fan at a rate of 18000±4000 $m^3$/day, outdoors and at ground level. The 30 cm × 30 cm filters were changed approximately daily, collapsed after removal from the fan, and inserted in front of a 45 cc Ge(Li) detector shielded for low-level background counting with 10 cm of lead. The Ge(Li) detector had a resolution of 1.6 keV at 500 keV. Spectra were accumulated usually over a one day period on a 4096 channel Nuclear Data ND2400 MCA with a hardware link to the VAX.

A spectrum taken from the air filter run between the evenings of May 1st and May 3rd detected $^{7}$Be, originating from cosmic-ray spallation reactions in the ionosphere, and daughters of the naturally radioactive $^{232}$Th and $^{238}$U alpha-decay chains. The spectrum from the air filter run between the evenings of May 3rd and May 5th was the first to show gamma ray emissions from $^{131}$I and $^{132}$Te. Peak activity was seen in the filter exposed between 1900 May 9 and 1900 May 10, 1986 and is possibly correlated with heavy rainfall in Seattle on that day.

Isotopic activity ratios can be used to grossly estimate the reactor run time (≈1 year), fuel composition (≈25% $^{235}$U/$^{238}$U), fission operation time (≈ April 22), and neutron flux (≈6×10$^{13}$ n/cm$^2$/sec). The temporal dependence of the radioisotope arrival rates can yield information on global weather patterns. Comparison with other sampling efforts on campus,[1] where particulate filters were backed with activated charcoal traps, allows the particulate mass distribution to be unfolded. The activities monitored throughout the month of May did not contribute any significant increase to the total radiation exposure.

### Reference:

1. Notably Prof. W. Zoller *et al.* in the Chemistry Dept. and Prof. A. Nevissi in Fisheries.

## 13.1 Calculation of Thick Target Resonance Yields

E.G. Adelberger and P.B. Fernandez

We have developed a computer code which calculates the thick target (p,γ) resonant yield. For a proton beam of mean energy $E_B$ incident on a target of thickness t atoms/cm², the number of γ rays produced per incident proton is given by[1]

$$Y[E_B] = t \int_{E_i=0}^{\infty} \int_{E=0}^{\infty} \sigma_{lab}[E_R,E] \ g[E_B,E_i] \ \eta[E,E_i] dEdE_i + Y_0$$

$Y_0$ is the non-resonant yield

$$Y_0 = A_0 + A_1 \times E_B$$

$\sigma_{lab}[E_R,E]$ is the Breit-Wigner resonant cross-section

$$\sigma_{lab}[E_R,E] = \frac{\pi \lambda^2 \omega \Gamma_{lab}^2}{[E-E_R]^2 + \frac{\Gamma_{lab}^2}{4}}$$

where $E_R$ is the lab energy of the resonance

$$\omega = \frac{2J+1}{[2J_1+1][2J_p+1]} \left[ \frac{\Gamma_p \Gamma}{\Gamma} \right]_{lab}$$

$g[E_B,E_i]$ accounts for the beam energy spread, assumed to be gaussian

$$g[E_B,E_i] = \frac{1}{(2\pi)^{1/2} \sigma_B} \exp\left[-\frac{[E_B-E_i]^2}{2\sigma_B^2}\right]$$

$\eta[E,E_i]dE$ is the probability that a proton incident at energy $E_i$ is found in the target with energy between E and E+dE. The proton energy loss Q per collision was assumed to be distributed as $1/Q^2$, $q_{min} < Q < Q_{max}$, where $Q_{max}$ is the energy loss in a head-on collision with a free electron and $Q_{max}$ depends on properties of the target. For the distance $\Delta x$ between collisions, a distribution function $e^{-\Delta x/\lambda}$, where $\lambda$ is the mean free path, was assumed. Using the Monte Carlo method, protons were followed through the target, and $\eta[E,E_i]dE$ was calculated as the average distance travelled by a proton while in the $(E_i-E)$ energy loss bin divided by the target thickness.

The code then performs the double integration to obtain $Y[E_i]$. We are including a fitting routine so that the parameters $\sigma_B,E_R,\Gamma_{lab}$, ω,$A_0$ and $A_1$ can be varied to fit experimental data. Our first use of this program will be for a final analysis of the $^{13}C(p,\gamma)$ resonance data discussed in last year's Annual Report.[2]

References:

1. R.E. Marrs, Ph. D. Dissertation, University of Washington (1975), ch. 5.
2. Nuclear Physics Laboratory Annual Report, University Washington (1985) p. 4.

## 13.2 Data Acquisition System

### H.P. Readdy and R.J. Seymour

The principal data acquisition system is a DEC PDP 11/60 with a CAMAC-based experiment interface controlled by a BiRa MBD-11 microcomputer. The 11/60 uses the RSX-11M operating system, an RL-01 and RL-02 disk drive, a 1600 bpi 75ips tape drive, a Printronix P-300 printer/plotter with a Trilog Tektronix hardcopy board, a DEC VT-11 graphics display and a Tektronix 4006 terminal. The CAMAC crate connects to twelve Tracor Northern TN-1213 ADCs, plus occasional LeCroy 2249As, 2251s and 2256As. We have 15 NPL-built 10 digit scalers connected to an IEEE-488 bus. The IEEE bus also connects to target arm angle readouts and beamline magnet controllers.

There were no significant expansions of the acquisition system's hardware this year.

To use the new RLO2 disk drive with minimal impact on the data collection system we patched, rather than upgraded, the 11/60's RSX11M v3.1 operating system.

Minor software enhancements included improvements in custom experiment programs, the line plotting program, the VT-11 display program and our version of MULTI. A change was made in QDA to include a "record number" in each tape record to help account for any data loss due to bad tapes.

We are still seeing rare crashes that appear to be MBD-11 caused. These occur only while using a particular MBD-11 program. They occur about once per day at about 1 A.M. The problem does not cause an immediate crash, but corrupts the 11/60's data structures so that later attempts to run programs fail. Their rarity makes diagnosis difficult. The VT-11 display program has been modified to watch for, report and "correct" known symptoms.

Another IBM PC-AT is now serving as part of a stand-alone data acquisition system (see Sec. 4.2).

****** 

## 13.3 Data Analysis and Other Systems

### J.R Longwill, H.P. Readdy, and R.J. Seymour

Our data analysis system consists of a 4 megabyte VAX 11/780 with 1 gigabyte of System Industries disks, two 75ips 1600 bpi tape drives and one 50 ips 6250 bpi drive, a Printronix P-300 printer/plotter, an HP 7475A pen plotter, an AED-512 color graphics display, two modems and thirty local terminals. It is connected via DECnet/Ethernet to the Booster console MicroVAX II.

*Hardware Developments:* The principal additions are a 6250 bpi tape drive and a DECnet/Ethernet connection to the MicroVAX II via a DEC DELNI. The MicroVAX serves as the human interface to control the booster systems. It has about 80% of the computational speed of the 11/780. During the development stage of the booster we put overnight batch jobs into the MicroVAX, with their datafiles still residing on the main VAX's disks (see Sec. 14.15). For programs requiring DEC's "G-format" floating point dynamic range, the MicroVAX runs ten times faster than the 11/780. Although the MicroVAX has only two megabytes of memory and 30 megabytes of disk space, the lack of competition for its cpu permits large batch jobs to execute in what they see as a better environment than our interactive-tuned 11/780. Likewise, the interactive jobs on the 11/780 stop seeing the impact of those same large batch jobs.

We have added a Telex 9251 "Shamrock" 6250 bpi, 50 ips tape drive on a Wespercorp Tape Dimension III controller. An imperfect emulation of the DEC TS11 controller was finally resolved by Wespercorp replacing the ROMs on the controller, thereby turning it into a Tape Dimension IV. Address conflicts on the UNIBUS necessitated removing the old Wespercorp TC-130 controller, thus making the seven track drive inaccessible. In the past year, we have reinstalled the TC-130 twice to recover data from tapes dating back to 1963.

*Software Developments:* A new VAX SINGLES tape/file utility has replaced the old VAX-compatible duplicate of our MAGUTL from the 11/60. The old one did not effectively deal with the VMS file structure, nor did it understand the expanded header forms produced by MUSORT and our spectrum analysis program HP.

Our spectrum analysis program HP was modified to allow for floating point "channel counts", to allow its use with program-generated spectra. Our other analysis programs MUSORT and VAXSPAN received maintenance work and some expansion based on user requests.

We modified SLAC's TOPDRAWER and UGS package to provide continuous output from our Printronix plotter, variable plotfile names and improved scaling. Some changes were made to improve performance under VMS 4.x, plus a DCL command file was written to allow the data to be merged with a separate "header" file to ease multiple plots of a common format.

We acquired an IBM PC-AT for use in mechanical drafting for the booster using AutoCAD. We have speeded up the IBM PC-AT by installing an 18 megahertz crystal in place of its original 12 MHz crystal. The system is often used 24 hours per day with people generating drawings throughout the night. It has provided a timely means for the booster drawings to be updated and redrawn as changes occur.

## 14.1 Construction of the Superconducting Booster Accelerator

J.F. Amsbaugh, M.K.M. Brown, R.S. Burton, R.C. Connolly, R.L. Cooper, D.T. Corcoran, J.G. Cramer, J.R. Cromie, J. Davis, J.G. Douglas, R. Durham, H. Fauska, R.W. Floyd, B.J. Fulton, L.L. Geissel, D.J. Hodgkins, B.P. Holm, M.A. Howe, T.J. Irwin, L.W. Jackson, J.A. Katterman, J.M. LaCroix, D.D. Leach, Q.-X. Lin, C.E. Linder, J.R. Longwill, J.-Q. Lu, T. Meadows, D.B. Newell, R.G. Ramirez, H.P. Readdy, B. Sanborn, R.J. Seymour, L. Sima, H. Simons, J.M. Stshfest, D.W. Storm, R.E. Stowell, H.E. Swanson, J.J. Tomasko, T.A. Trainor, R. Vandenbosch, L.P. Van Houten, T.D. Van Wechel, W.G. Weitkamp, D.I. Will, and A. Willman

The superconducting booster accelerator is expected to produce proton energies of 36 MeV and energies of up to 20 MeV/A for the lighter heavy ions dropping to 10 MeV/A around mass 40. Quarter wave resonators were chosen to optimize the range of masses that could be effectively accelerated. The linac will consist of 36 superconducting resonators in 12 large cryostats plus two resonators operating as bunchers in two smaller cryostats.

During the past year we have moved out of the design phase into an intense period of construction, installation, and assembly. We have completed many components of the accelerator and a large fraction of the laboratory's effort has gone into their installation and testing. In the course of this work we have surmounted an interesting spectrum of the sorts of problems which are normal to a project of this size. In general the work has proceeded smoothly on all fronts.

In addition, we have completed successfully our prototyping of the high beta resonators and are starting to produce these. These resonators are designed to operate for higher particle speeds ($\beta$=0.2) than those of other tandem boosters because of our interest in accelerating the very lightest ions. It was therefore necessary for us to develop these high $\beta$ resonators on our own. We find that they perform as well as (or better) than the smaller resonators optimized for velocities of 0.1 c.

We have completed construction of all the low beta resonators and have plated about half of them. A buncher cryostat and four accelerator cryostats containing low beta resonators have been installed. Along with those cryostats we have installed appropriate magnets and parts of the control system. Each of these cryostats with its associated equipment represents a module of the accelerator. Together, they comprise more than 1/3 of the complete accelerator. Soon we will be able to use them with the beam for serious tests of the accelerator system, while at the same time we will continue to install the remaining parts of the machine.

The low energy buncher has been completed and tested, and the dogleg beam transport system, as well as the beam transport through the high energy buncher to the first cryostat, have been installed and tested successfully using the beam. All of the appropriate diagnostic elements are included in these beam transport sections.

Much of the control system is ready for use, and the satellite controllers are being used to control resonators and magnets. The major components for the injector deck have been tested successfully and delivered, and installation is taking place.

The helium refrigerator has been run regularly, and the first part of the cryogenic distribution system has been delivered and is being installed. The refrigerator capacity is about double that needed to handle all the measured heat loads of the accelerator running at the design accelerating field. The final installation of the utilities is now taking place, and we are able to use them for the parts of the accelerator that have already been installed.

So far, we have cooled the buncher cryostat and the first accelerator cryostat by batch transfer, and have operated the resonators at liquid helium temperature. However, we have not yet operated the resonators with the beam present. As soon as the helium distribution system is commissioned, we will begin running the resonators in the first cryostats in tests with beams. We are looking forward to testing an entire subsection of the accelerator with the beam during June of 1986. We still plan (as we have from the beginning of the project) to finish installing the accelerator by the end of 1986 and to continue debugging and testing during the first half of 1987.
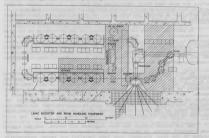


LINAC BOOSTER AND BEAM HANDLING EQUIPMENT

**Fig. 14.1** Layout of the accelerator. The shaded parts indicate equipment which has been installed as of June 1, 1986.

## 14.2  Building Modifications

C.E. Linder, W.G. Weitkamp, and D.I. Will

To install the booster, modifications had to be made to the Laboratory building electrical service, cooling water system, air conditioning and shielding.

*Electrical service:*  The building is served by three phase power at two voltages, 208 V and 460 V, each from a 500 kVA transformer.  Completion of the booster will bring the 460 V load to 745 kVA.  Most of this new load drives the helium refrigerator compressors.  To cope with the new load and also to get rid of a PCB filled transformer, the old transformer was replaced by a 1000 kVA transformer.  Four new circuit breaker panels were also to added to make both 208 V and 460 V power accessible to the booster and the helium refrigerator compressors.

*Cooling water:*  All of the electrical energy used by the booster must be removed from the accelerator vault, primarily by water cooling power supplies.  The existing tandem cooling water system did not have adequate reserve capacity to provide this cooling.  A cooling water system with a cooling tower has been installed with provisions for maintaining the water at a high resistivity to minimize corrosion and stray currents.

*Air conditioning:*  We expect approximately 45 kW of power to be dissipated in the air of the accelerator vault.  It is not feasible to increase the capacity of the existing air conditioning system.  To solve this heat problem, fan-coil units were hung along the walls of the vault, using chilled water from the building refrigeration system, which has some spare capacity, to cool the air over the booster pumps, compressors and RF amplifiers.

A consultant, Elcon Associates, designed and supervised installation of electrical, cooling water and air conditioning systems to meet the needs of the booster.  All the equipment has now been installed and has passed acceptance tests.

*Shielding:*  In order to keep research going on the tandem accelerator while the booster is being installed, it is desirable shield the booster area from radiation produced by the accelerator.  We have installed a precast concrete block wall 3 ft thick by 7 ft high across the accelerator vault.  Although this wall is not high or thick enough to shield completely against neutrons produced by beams of high energy protons or deuterons, it permits personnel to work in the booster area most of time that the accelerator is operating.

The resonators of the booster produce x-rays when conditioning and when operating at high fields.  Measurements show that 3" of iron shielding is adequate to reduce the x-ray flux from the low β resonators to an acceptable level and 4" of shielding is required for the high β resonators.  These shields have been installed.

65

14.3  Radiation Safety System

H. Fauska, C.E. Linder, and W.G. Weitkamp

To accommodate the booster, the radiation safety system at the accelerator will require major modification. The existing system[1] combines several important features. Bonner spheres and ion chambers comprise the neutron and gamma ray sensors for this system. These sensors produce audible clicks at the rate of 1 click/sec = 1 mrem/hr. This clicking sound provides the first level of warning of radiation danger. This rate of clicking has an important psychological effect because 100 clicks per second, corresponding to the dose equivalent at which a "radiation area" becomes a "high radiation area", gives a strong signal of danger.

The accelerator area is divided unto 4 zones. When the dose equivalent at a sensor in one of the zones exceeds 100 mrem/hr, an interlock relay contact is closed. The high radiation relay contact is monitored by a programmable controller which also monitors all doors and barriers in the accelerator vault. When a high radiation relay contact is closed in a zone, the programmable controller shuts off the beam unless all doors and barriers allowing entry into the zone are closed.

Installation of the booster adds three new zones: the south row of cryostats, the north row of cryostats and the region of control electronics in between. It is also possible that booster accelerated deuteron beams may slightly exceed environmental radiation limits outside the accelerator building.

We have bought Bonner spheres and gamma-ray monitors to install in the new zones and a new programmable controller to carry out the logical operations required. We will also install a Bonner sphere to monitor neutron levels outside the building.

The status of all door and barrier interlocks and radiation monitors around the accelerator will be displayed on a board in the control room. This board will be operated directly by the new programmable controller so that the radiation safety system will be completely independent of the VAX computer which controls the operation of the booster.

Except for the Bonner spheres, all equipment for this system is in hand. Wiring and modification of the radiation monitors to make them compatible to our system is under way.

Reference:

1. Nuclear Physics laboratory Annual Report, University of Washington, 1968 p. 68.

******

## 14.4  Successful Development of β=0.21 Resonators

J.F. Amsbaugh, D.T. Corcoran, M.A. Howe, and D.W. Storm

In last year's Annual Report[1] we described the design and unsuccessful construction and testing of the high beta (β=0.21) resonator. We have published more detailed reports elsewhere.[2] During the past year we have been able to repair the cracked welds and to achieve successful tests of that resonator and a second one. In one case this repaired weld was quite rough. The plated resonator was tested and performed adequately. To improve performance, we ground off the rough spots, then the resonator was replated and the test results were excellent.

The test results are shown in Fig. 14.4. The results for resonator #1 were obtained after the weld was ground smooth. For both resonators we obtain fields comparable to those attainable with the low beta resonators using less than twice their power. As the resonators are twice the diameter of the low beta resonators, one would expect to require twice the power (excluding field emission losses).
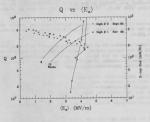


Fig. 14.4 The points show Q vs the average accelerating field for two high beta resonators. The curves connecting points show x-ray flux (which results from field emission) vs accelerating field.

References:

1. Nuclear Physics Laboratory Annual Report, University of Washington (1985) p. 77.

2. D.W. Storm, J.M. Brennan, and I. Ben-Zvi, IEEE Trans Nucl. Science NS-32 (1985) 3607; D.W. Storm, J.F. Amsbaugh, D.T. Corcoran, and M.A. Howe, Proceedings of 1985 SNEAP, Rev. Sci. Instrum. 57, 773 (1986).

## 14.5 Resonator Production Status

### Mark A. Howe

The booster production run of the low beta resonators came to an end in early May with the brazing of resonator #29. This gives the booster project its total complement of 25 low beta resonators with three spares. This number does not include the two prototypes and the resonator that was sold to the Tata Institute in Bombay, India. The production of the needed thirteen high beta resonators has begun.

Various difficulties were noted during the low beta production run, none of which caused serious problems. Two resonators (#4,#13) developed cracks on the weld between the interior center conductor and the outer conductor and had to be rewelded. Because the cracks were noted after the high temperature drift tube brazing operation, the brazing cool-down procedure was changed to put less stress on the weld joint. There have since been no cases of cracked welds.

Two resonators (#7,#8) had leaky conflat flange unit welds. These were fixed by soldering a copper patch over the leak. To prevent future problems the e-beam welding procedure was changed to put a wide cosmetic weld over the structural conflat flange unit weld. Since then none of the conflat welds have leaked.

Two other resonators (#16,#21) had a failed drift-tube braze joint. No reason could be found for these failures. The bad drift tubes were removed and new ones brazed in place.

All of the high beta material is in hand and substantial machining has already been done. All of the tuning plates, conflat flange units, and tuning plate attach rings were finished by mid April. In addition, machining of the center conductors and outer conductors is well under way with an anticipated completion date of June for the first four resonators.

******

14.6  Plating Experience

D.T. Corcoran

In 1985, we successfully plated two high-beta resonators and five low-beta resonators. The success rate for the high-betas was about 25%, for the low-betas about 50%. Some experimenting was done with thin plating (about two microns) but no reliable results were obtained. The two most persistent problems were poor welds between the center conductor and the outer conductor and thin copper foil deposited during the electron beam welding. The welds often had small pits or cracks in them that trapped plating fluids that later etched the lead surface. This problem was solved by taking more care with the welding. The inadequate foil removal problem was solved by tumble polishing. The resonators are now polished by filling the resonators with different grades of plastic and glass abrasive media, then tumbling for 48-72 hours. This gives a much more uniform and reproducible finish than polishing by hand.

In the first five months of 1986 we have successfully plated 18 low-beta resonators with a success rate of about 75%. This rate seems to have increased with the addition of vibratory agitation to the plating process and a closer watch on additive depletion. To date 17 resonators have been installed in cryostats.

******

14.7  Cryogenic System

M.K.M. Brown, R.L. Durham, J.R. Longwill, W.G. Weitkamp, D.I. Will, and J.A. Wootress

During the past year the Koch 2830 S helium refrigerator has operated 4000 hours under light loads. We have encountered no major problems.

Janis Research has completed construction and testing of nine of fourteen cryostats. Seven have been received and five loaded and installed. We are plagued by instrumentation feedthroughs which develop small vacuum leaks when their conflat flanges are tightened and by rotary feedthroughs which will not operate at manufacturer's (not Janis) rated torque. The cryostats themselves perform well from a cryogenic standpoint but we have not accelerated beam through them yet.

Part I of our cryogenic distribution system is installed and is being debugged. It supplies the buncher and first two cryostats with liquid helium and liquid nitrogen and returns cold helium vapor to the refrigerator cold box. The next line segment is ready for testing at Beech Aircraft, Boulder Division. Beech is completing the final line segment and hopes to test it during June, 1986. Tests of part I at Beech indicate performance consistent with our specified maximum total heat leak to helium of 50 watts (for the whole distribution system.)

14.8 Vacuum Systems and Beamline Installation

J.G. Amsbaugh, J.A. Katterman, and J. Davis

During the last year, installation of the booster linac vacuum system has progressed. This system has been described in previous reports.[1] To date, the buncher cryostat and the first four accelerator cryostats have been installed along with their associated pumping systems - 360 1/sec turbo-molecular pumps. The three beamlines needed to transport beam from the tandem to the linac have been installed. The first, the dogleg magnet chambers, are pumped by two 20 1/sec ion pumps. The second, which connects the dogleg to the buncher, will not pumped until later. The third, which connects the buncher to the first accelerator cryostat, is pumped with a 150 1/sec turbo-molecular pump with a 14 CFM forepump. Pressures are $1-5\times10^{-7}$ Torr in beamlines and around $5\times10^{-6}$ Torr in the cryostats before cooling, but are $3\times10^{-8}$ Torr after the liquid nitrogen heat shield is filled. Temporary switch panels have been used to control the pump stations while the vacuum control computer system was being built.

The vacuum control computer is a LSI 11/23 in a Q-bus crate. The current configuration has 256 status inputs, 160 control outputs, and 96 ADCs. This information is displayed on a 19" color monitor equipped with a touch screen for operator input. A list processor control program has been developed so that changes in the system, interlock overrides, and installation do not require rebooting a new control program which would shut the entire vacuum system down.

The interface between the I/O boards and the various devices must present an orderly relation between computer address and the terminal strips connected to the device. The interface must also be isolated electrically to avoid ground loops. The output interface consists of an array of solid state relays. It monitors the data valid line from the computer. If the data valid signal is missing for longer than 16 msec the outputs are all latched off. The devices controlled are "safe" in the off mode. The input interface means device status when the input line is connected to computer ground by relays and/or switches in the device. The ADC interface has an array of unity gain instrumentation amplifiers to isolate the local ion gauge controller ground from the computer ground. This interface hardware has been completed and tested.

Reference:

1. Nuclear Physics Laboratory Annual Report University of Washington (1985) p. 86.

70

14.9 Injector Deck Status

J.G. Douglas, T.A. Trainor, and L.P. Van Houten

Major components are now arriving at the laboratory, and assembly of the deck has begun.

In early April Glassman High Voltage announced that it had achieved a 6V p-p noise figure for its specially modified 300 kV switching power supply, thereby exceeding our 10V p-p specification. The power supply was shipped to Madison, Wisconsin for injector deck tests at NEC. There one of us (L.P. VH) confirmed the 6V performance with the deck attached. Deck and power supply were then shipped to the NPL where the deck is now being permanently installed.

Also in early April the 300 kV isolation transformer (3Φ, 30 kVA) was delivered by Hipotronics.

All vacuum and beam diagnostic equipment (Leybold-Heraeus, NEC) has been delivered. Ion source power supplies and electronics racks are expected by the end of May. The double-focussing 90° analyzing magnet is to be shipped in June.

Control system hardware, AC distribution, and detailed electronics rack layouts have been designed.

Deck ion optics centers around the 90° magnet conjugate foci. Because of space limitations, the beam-defining slits (object and image) are not at the actual magnet foci. The displacement of the slits is compensated by one or two 10 cm einzel lenses and an electrostatic quadrupole doublet depending on the ion source selected. Provision is made for three ion source stations at ±45° and 0° with respect to a switch magnet (expected August, 86). Each ion source has an object slit, and the common image slit is remotely controlled to change mass resolution or beam intensity. The image slit forms an object for the 300 kV acceleration tube supplied by Peabody/Dowlish and delivered in March.

Because of the expected late arrival of the switch magnet the existing direct extraction ion source will be moved to the 0° station when the deck is ready for tests. After the switch arrives the existing sputter ion source will be moved to the L45° station. The R45° station is available for future installation of a high-intensity heavy ion source.
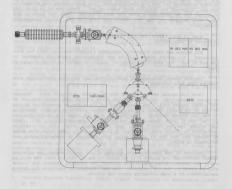
71

**Fig. 14.9  Injector deck plan view.**

## 14.10 Linac Control System

R.S. Burton, J.M. LaCroix, D.B. Newell, H.P. Readdy, R.J. Seymour, J.M. Stehfest, R.E. Stowell, H.E. Swanson, and T.D. Van Wechel

*Resonator controllers:* Design modifications have been made to the resonator controller.[1] The positions of an amplifier and directional coupler in the RF section were interchanged. This removes the need for a narrow band transformer in the amplitude detector and increases the signal level to the phase detector which should improve the phase performance of the resonators. The gain of the RF loop is also increased allowing self excited operation of warm resonators including conditioning. About 1/4 of the 40 completed controllers are of the previous design and are being modified.

*Satellite control stations:* Computer based satellite stations operate the resonator controllers. The satellites are the remote node for operation from the main control console and also have local control and monitoring capabilities. The completed linac will have 9 satellites including one for controlling the vacuum system, and one for cryogen distribution control.

The first and second low beta satellites have been installed and used to check out the resonators in the first four cryostats. The final low beta satellite station is presently being installed. The software for the resonator control satellites is essentially complete requiring only occasional modifications as additional capabilities are installed.

The vacuum system control satellite has been discussed in Sec. 14.8.

The computer for the cryogenics satellite is operational and software for manual control of the various cryogen valves has been written. The graphics menus for local operation using a touch screen have also been programmed. The system will be installed after completion of the hardware interface to the cryogenics distribution system.

The buncher satellite station has been installed and we have used it to operate the first buncher resonator. In addition, this satellite is being used for control and monitoring of the doglet magnets, and diagnostic devices used throughout the linac.

*Main control console:* The console relay rack and desk unit have been installed along with the graphics monitors and DEC MICROVAX II computer. There is an Ethernet connection between the Microvax II and the VAX 11/780. Using DECnet, beam transport calculations for the linac can be run on the Microvax while it functions as a control console. Many aspects of the console are now operational using graphics menus and the touch screens. The software which operates the console is described in Sec. 14.11.

### Reference:

1. I. Ben-Zvi, M. Birk, C. Broude, G. Gitliz, M. Sidi, J.S. Sokolowski, and J.M. Brennan, Nucl. Instrum. Methods, $\underline{A245}$, 1 (1986).

## 14.11 Master Control Program Status

Mark A. Howe

A preliminary version of the booster master control program is now up and running on a MicroVAX II. The master control program's purpose is to provide an easy to use man-machine interface to the booster and to coordinate the activities of the cryogenic, vacuum, resonator, and injector deck satellite control computers.

The MicroVAX computer is running the MicroVMS operating system, has a thirty megabyte hard disk, and currently contains two megabytes of random access memory. The control interface is via two high resolution color monitors equipped with touch sensitive screens. Communication to the satellite computers is via a RS232 network.

The control software is written in the 'C' language and is completely interrupt driven to provide low computational overhead and real time response. The operator interface is provided by displaying various graphic menus containing schematic views of booster hardware and/or data. By touching the picture on a monitor the operator can change menus, turn equipment on or off, change parameter values, or examine critical data. Using computer generated graphics in this way gives the booster a 'virtual' control panel which can be easily changed or updated.

The system consists of four concurrently running processes:

1) The command interpreter. This routine monitors the console terminal for commands, does the command parsing, and checks for proper command syntax.

2) The command dispatcher. This program serves as a clearing house for inter-process communication and handles all messages going out to the satellite computers.

3) The satellite message interpreter. All incoming satellite messages are received and interpreted by this routine. It also keeps a data base of all satellite parameters.

4) The touchscreen control program. This program drives the two touch screens to monitor the touch sensitive areas of the monitors, switch between graphic menus, and update displayed data in real-time.

The system that is currently running completely supports communication with the resonator control satellites and can be used to set quadrupole and dipole magnet currents. Work continues to provide cryogenic, diagnostic, vacuum, and injector deck controls.

\*\*\*\*\*\*

## 14.12 Adjustment and Bunching Test of the Low Energy Buncher

J.P. Amsbaugh, D.D. Leach, Q.-X. Lin, D.W. Storm, and T.D. Van Wechel

The prebuncher control system was completed in December, 1984 and the buncher construction was completed in March, 1985.[1] Between then and the end of the same year, the buncher was adjusted, improved and used for doing beam bunching tests on the tandems.

(a) Adjustment of the Buncher. Initially, the buncher could not resonate at the four harmonic frequencies at the same time. This problem was resolved by changing the connecting mechanism between the center conductor of the coaxial resonant line and the grid, from a short and straight line to a longer and curved one.

A computer program simulates the actual tuning procedure of the buncher, estimates its resonant frequencies and proposes the optimum tuning parameters.

A buncher's Q equation was deduced to analyze various kinds of factors which affect the buncher's Q. The calculated Q agrees with the measured Q. The gap between the mounting structure of the grids was widened from 1.0 mm to 1.9 mm. The buncher's Q at the fundamental frequency was improved from 500 to 700.

(b) Bunching Test of the Buncher. A sawtoothlike waveform of the buncher has been combined from the four harmonic frequencies. The correct relative phase among the four harmonic frequencies was set by observing the arrival time of bunches made by each harmonic used alone. By driving the buncher at various voltages with each harmonic and observing the bunch shape, it was possible to calibrate the amplitudes.

More than 70% of 46 Kev proton DC beam has been bunched in 1 ns wide pulses. The control system works stably. It will be necessary to make some adjustments in order to bunch ions from the high voltage injection deck.

Reference:

1. Nuclear Physics Laboratory Annual Report, University of Washington (1985) p. 89.

******

R.C. Connolly, H. Fauska, M.A. Howe, T.J. Irwin, D.D. Leach, H.P. Readdy and W.G. Weitkamp

Tuning the beam through the booster and diagnosing problems requires a set of beam diagnostic instruments consisting of beam profile monitors, slits, Faraday cups, beam energy monitors, a time structure monitor, and emittance measuring devices.

These devices will be controlled by the buncher satellite computer from instructions entered into the main control computer via the touch screens. The network of switches, readouts and stepping motor drivers to control the diagnostics has been planned and several components of this system have been completed.

Most of the diagnostics between the tandem and the first cryostat are now installed and tested, using a temporary manual control system.

*Beam profile monitors:* We are using NEC rotating helical wire type beam profile monitors. All monitors have been delivered and about half have been installed. A readout system based on an Argonne National Laboratory design which displays the vertical trace vertically and the horizontal trace horizontally has been completed.

*Slits:* Custom made slits will be required in three locations because of space limitations. Two of these slits have been completed and installed.

*Beam energy monitor:* Three beam energy monitors will be installed. Each consists of a scattering foil and a solid state detector. These will be installed at the entrance to the linac, at the end of the south row of cryostats and at the exit of the linac. The monitor at the linac entrance will be in the second stripper foil housing. Two of the three monitors have been completed and most parts are on hand for installation. We are purchasing a stand-alone pulse height analyzer to display the output of these devices.

*Time structure monitor:* A time structure monitor is used to measure the time shape of the beam bunches entering the linac. It is located at the time focus of the high energy buncher. A microchannel plate detector, together with appropriate fast electronics, will be used to detect either scattered beam or secondary electrons from a foil or wire inserted into the beam. The detector and electronics are in house and experiments are in progress to determine a suitable detector housing design.

*Emittance measuring device:* An emittance measuring device moves a slit both horizontally and vertically across the beam. At each position the beam current distribution perpendicular to the slit is measured at a short distance from the slit. A computer generates a plot of slit position vs. beam divergence for each scan. We plan to locate one of these devices before the booster and one after the last resonator.

14.14  Resonant Phase Detector

R.C. Connolly

A quarter wave resonator tuned to the pretandem buncher[1] frequency of
49.6 MHz has been built to provide a phase locking signal[2] for the buncher.
It is similar to a resonator used at SUNY, Stony Brook.[2] The resonator cavity
is a Cu cylinder of inside diameter 10.2" and inside length 9.5". A 1"
diameter beamline lies along the cylinder axis. This beamline consists of two
1.5" long re-entrant drift tubes and a 4.5" long center drift tube. Teflon
cylinders with Viton O-ring seals span the two 1" gaps. Only the beamline is
under vacuum. A three turn helix formed from Cu tubing with a pitch diameter
equal to half the cavity diameter is coaxial with the beam tube. One end of
the helix is soldered to a post attached to the center drift tube, and the
other end is soldered to a post attached to the outer wall.

The resonator is located immediately after the high energy buncher. It
is driven by the pulsed beam from the tandem. A signal is extracted by a loop
of wire at the base of the conductor post. The signal is amplified by an
automatic gain control amplifier which is similar to one developed at SUNY,
Stony Brook.[3] The amplifier output varies from 11.0 dBm to 12.3 dBm as the
input goes from −74 dBm to −34 dBm.

The resonator and amplifier have been tested with a beam of 16.1 MeV
protons in which 85% of the beam was in 2 ns wide bunches. A signal which
should be usable for phase locking the buncher was measured down to a beam
current of 13 nA. The resonator has not yet been used to phase lock the
pretandem buncher.

This resonator is considered to be a prototype. We are planning to
build a high vacuum resonator employing metal gaskets and metal-to-ceramic
seals.

References:

1. Nuclear Physics Laboratory Annual Report, University of Washington (1985)
   p. 89.
2. Nuclear Physics Laboratory Annual Report, University of Washington (1984)
   p. 98.
3. J.M. Brennan, private communication.

******

## 14.15 Linac Beam Dynamics Studies

J.G. Cramer, J.-Q. Lu, and D.W. Storm

(a) *Beam Transport Magnets:* The beam transport magnets for the dogleg system between the tandem and linac have been received from Magnecoil, slightly modified, and installed. The dogleg system has been successfully tested with beam, and feedback control of the tandem with signals from the dogleg slit system was accomplished without difficulty. The three beam transport quadrupoles have been received from Brucker, and one of these has been installed and tested with beam. Twelve high gradient inter-resonator quadrupole doublets have been received from Danfisik and six have been installed. A second order for two more of these quadrupoles has been placed with Danfysik. An order for the 180° and 90° magnet systems has been placed with Brucker. Three pre-cast concrete stands for the dipoles of these systems have been designed and ordered.

(b) *Beam Dynamics Calculations:* We have continued with beam dynamics calculations for the booster. Comparisons of the predictions of the beam dynamics programs TRANSPORT, LYRA, and ENTIME were made to insure that equivalent calculations produced equivalent results. Several minor errors and inaccuracies in the latter two codes were detected and corrected by this procedure. The search features of TRANSPORT have been used to generate transport matrices which can be used as input for LYRA, permitting excellent simulation of magnet and linac characteristics. This approach has been used to model the transport of representative beams through the system. We have given particular attention to beam size during acceleration and to the debunched energy resolution of the final beam. Fig. 14.15 shows the horizontal and vertical width of a $^4He^{2+}$ beam as it passes through the magnet and linac system. Typical predicted beam diameters in the linac are a few millimeters. These calculations indicate the following FWHM time and energy widths for selected beams: p(260 ps, 29 keV), d(69 ps, 37 keV), $^4He$(59 ps, 29 keV), and $^{12}C$(340 ps, 70 keV).
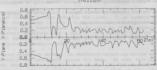


Fig. 14.15 Helium beam size in horizontal (x) and vertical (y) directions as a function of distance (z) along the linac.

D.W. Storm, T.A. Trainor, and L.P. Van Houten

Installation of the 300 kV injector deck requires additional ion optic elements as well as replacement of some existing elements in order to transport the higher energy ion beams to the tandem accelerator.

The revised low energy beam transport system is shown in Fig. 14.16. The beam from the 30 kV deck acceleration tube emerges with low divergence and enters the first of two electrostatic quadrupole triplets with focal length ~ 40" at 7 kV and 2.3" aperture. This lens forms a waist between 50" and 150" downstream and acts, with the second electrostatic lens just before the tank base, as a telescope in order to provide good matching to the accelerator acceptance.

A faraday cup and scanner will be placed approximately half way between the acceleration tube exit and the first quadrupole. Magnetic x-y steering will be provided at the acceleration tube exit and at the cup/scanner combination. Although this is a mass-dependent optical element we expect any substantial steering requirement to be removed by mechanical realignment of the optical system.
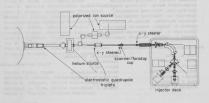


Fig. 14.16 Revised tandem injection optics.

## 15. APPENDIX

### 15.1 Nuclear Physics Laboratory Personnel

#### Faculty

Eric G. Adelberger, Professor
David Bodansky, Professor
John G. Cramer, Professor; Director, Nuclear Physics Laboratory
George W. Farwell, Professor
Pieter M. Grootes, Joint Senior Res. Assoc., Geological Sciences
I. Halpern, Professor
Eric B. Norman, Affiliate Assistant Professor[1]
Fred H. Schmidt, Professor
Kurt A. Snover, Research Professor
Derek W. Storm, Senior Research Scientist;
   Director, Superconducting Booster Project
Thomas A. Trainor, Research Associate Professor
Robert Vandenbosch, Professor
William G. Weitkamp, Research Professor; Technical Director,
   Nuclear Physics Laboratory

#### Research Staff

Ilan Ben-Zvi, Visiting Scientist[2]
Cynthia A. Gossett, Research Associate
Marta Kicinska-Habior, Visiting Scientist
Munther Hindi, Visiting Scientist[3]
Balakrishna Kurup, Visiting Scientist[4]
Qui-Xun Lin, Visiting Scientist[4]
Jian-Qin Lu, Visiting Scientist[5]
Tetsuya Murakami, Research Associate[6]
Martin J. Murphy, Research Associate[7]
Christoph C. Sahm, Research Associate[8]
Daniel R. Tieger, Research Associate[9]

#### Predoctoral Research Associates

| | |
|---|---|
| John A. Behr | Mahbubul A. Khandaker |
| Keith J. Davis | Russell Owen[10] |
| Gerald Feldman | Amlan Ray[11] |
| Patricia Fernandez | Douglas Rosenzweig |
| Holger K. Glatzel | Christopher Stubbs |
| Jens H. Gundlach | Peter Wong |
| Stephen E. Kellogg | Valdis J. Zeps |

## Professional Staff

John F. Amsbaugh, Research Engineer
David Balsley, Research Engineer
Roger C. Connolly, Research Engineer
Jim Davis, Research Engineer
J. Greg Douglas, Visiting Controls Engineer[1,2]
Harold Fauska, Senior Research Scientist[13]
Gervas M. Hinn, Research Scientist/Target Maker
Robert D. Hobbs, Research Engineer
David J. Hodgkins, Research Engineer
Mark A. Howe, Research Engineer
Donald D. Leach, Research Scientist
H. Pamela Readdy, Computer System Engineer
Richard J. Seymour, Computer System Manager
Rod E. Stowell, Electronics Engineer/Electronic Shop Supervisor
H. Erik Swanson, Research Physicist
Louis P. Van Houten, Research Engineer
Timothy D. Van Wechel, Electronics Engineer
Douglas I. Will, Research Engineer

## Technical Staff

Robert L. Cooper, Instrument Maker
Dean T. Corcoran, Engineering Technician
James R. Cromie, Accelerator Technician
Robert Durham, Accelerator Technician[10]
Louis L. Geissel, Instrument Maker, Student Shop Leadman
Brian F. Hoin, Instrument Maker
John M. LaCroix, Electronics Technician
Carl E. Linder, Engineering Technician
George E. Saling, Accelerator Technician[13]
Laurence Sims, Drafting Technician[10]
Byron A. Scott, Instrument Maker[10]
Hendrik Simons, Instrument Maker, Shop Supervisor
John M. Stehfest, Electronics Technician
Jay J. Tomasko, Accelerator Technician
John A. Wootress, Accelerator Technician
Allen L. Willman, Instrument Maker[13]

## Administrative Staff

Ronald Floyd, Buyer
Barbara J. Fulton, Administrative Secretary
Holly L. Johnson, Office Assistant
Margaret M. Nims, Office Assistant[10]
Maria G. Ramirez, Program Assistant

## Part Time Staff

Robert Abel[10]                    David Badt
James Annis                        Frederick L. Bahr
Darrell Armstrong                  Donald W. Black

Margaret K.M. Brown
Richard Burton
David Chan[1]
Tony F. Diego[10]
Steven P. Doub
Jane Fuller[1]
Albert Herron
Norman Hill[10]
Timothy J. Irwin
Darrel Isbell[10]
Lee W. Jackson
Peter James[10]
James Katterman[1]
Robin Kletke[10]
James R. Longwill

Gary S. Malkasian
Henry McDonald
Kevin McMurry
Thomas A. Meadows
Denton K. Morris
Eric Muller[10]
David B. Newell
L. Thomas Nirider
Joseph R. Olson
Darren Paschke
David Patterson[10]
Robert Rose
Barbara Sanborn
Jeff Stodola
Rob Vander Stoep
Eugene Wong[10]

---

1. Address: Lawrence Berkeley Laboratory, University of California, Berkeley, CA 94720.
2. Permanent Address: Department of Nuclear Physics, Weizmann Institute of Science Rehovot, Israel.
3. Permanent Address: Tata Institute of Fundamental Research, Bombay India.
4. Permanent Address: Peking University, Peijing, People's Republic of China.
5. Permanent Address: Peking University, Peijing, People's Republic of China.
6. Now at: NSCL/Cyclotron Laboratory, Michigan State University, East Lansing, MI 48824-1321
7. Now at: Lockheed Palo Alto Research Laboratory, Palo Alto, CA 94304.
8. Now at: Stiftstr. 36, 6050 Offenbach am Main, Federal Republic of Germany.
9. Now at: Bates Linear Accelerator Center, M.I.T., Cambridge, MA 02139.
10. No longer associated with the Nuclear Physics Laboratory.
11. Now at: Cyclotron Institute, Texas A&M, College Station, TX 77843.
12. Permanent Address: Group 3 Technology Ltd., Auckland, New Zealand.
13. Retired - part time employee.

******

14.2 Ph.D. Degree Granted, Academic Year 1984-1985

"Orbiting in Light Heavy Ion Reactions," A. Ray, Ph.D. Thesis, University of Washington, 1986.

## 14.3 List of Publications

*Published Papers*

"Parity Violation in the Nucleon-Nucleon Interaction," E.G. Adelberger and W.C. Haxton, Ann. Rev. Nucl. Part. Sci. 35, 501 (1985).

"A Simple Production Method for Making 3 μg/cm² Cracked Slacked Carbon Accelerator Stripper Foils," G.M. Hinn, 12th World Conference of the INTDS, Antwerp, Belgium, 1984 (invited paper); Nucl. Instrum. Methods 236A, 572 (1985).

"Nuclide Distributions for Fe-Like Fragments in the $^{136}$Xe+$^{56}$Fe Reaction," D.K. Lock, R. Vandenbosch, K. Lesko, S. Gil, A. Seamster, D. Leach, and A. Lazzarini, Nucl. Phys. A 442, 142 (1985).

"Cross Sections Relevant to Gamma-Ray Astronomy: Alpha-Particle-Induced Reactions on $^{12}$C, $^{14}$N, and $^{16}$O Nuclei," P. Dyer, D. Bodansky, D.D. Leach, E.B. Norman, and A.G. Seamster, Phys. Rev. C 32, 1873 (1985).

"Decay of Excited Projectile Residue into Complex Fragments," M.J. Murphy, D. Leach, A. Ray, A. Seamster, and R. Vandenbosch Phys. Rev. C 33, 165 (1986).

"Low Energy π⁻ Inelastic Scattering from Nuclei to the Continuum," K.A. Aniol, D.T. Chiang, K.G. R. Doss, I. Halpern, M. Khandaker, D.W. Storm, D. R. Tieger, P.D. Barnes, B. Bassalleck, N.J. Colella, J.A. Dytman, R.A. Eisentein, R. Grace, C. Maher, D. Marlow, P. Pile, R. Rieder, F. Takeutchi, and W.R. Wharton, J.F. Amann, and J. Julien, Phys. Rev. C 33, 208 (1986).

"Does the Cabibbo Angle Vanish in Fermi Matrix Elements of High J States?" E.G. Adelberger, P.B. Fernandez, C.A. Gossett, J.L. Osborne, and V.J. Zeps, Phys. Rev. Lett. 55, 2129 (1985)

"Anomalously Broad Spin Distributions in Sub-Barrier Fusion Reactions," R. Vandenbosch, T. Murakami, C.-C. Sahm, D.D. Leach, A. Ray, and M.J. Murphy, Phys. Rev. Lett. 56, 1234 (1986)

"The Transactional Interpretation of Quantum Mechanics," J.G. Cramer Rev. of Mod. Phys. 58, (1986).

"A Computer Program for Predicting Tandem Parameters," Report to SNEAP 1985, W.G. Weitkamp, in Proc. of the Symposium of Northeastern Accelerators Personnel, 1985, Rev. Sci. Instrum. 57, 740 (1986).

"Status of the University of Washington Superconducting Booster," Report to SNEAP 1985, J.F. Amsbaugh, R.C. Connolly, D.T. Corcoran, J.G. Cramer, M.A. Howe, D.W. Storm, H.E. Swanson, T.A. Trainor, R. Vandenbosch, L.P. Van Houten, W.G. Weitkamp, and D.I. Will, in Proc. of the Symposium of Northeastern Accelerators Personnel, Rev. Sci. Instrum. 57, 761 (1986).

"Superconducting Tests of Beta=0.1 and Beta=0 Resonators, Report to SNEAP 1985, D.W. Storm, J.F. Amsbaugh, D.T. Corcoran, and M.A. Howe, in Proc. of the Symposium of Northeastern Accelerators Personnel, Rev. Sci. Instrum. 57, 773 (1986).

"The NPL Superconducting Linac Control System," Report to SNEAP 1985, H.E. Swanson, M.A. Howe, L.W. Jackson, J.M. LaCroix, H.P. Readdy, D.W. Storm, and L.P. Van Houten, in Proc. of the Symposium of Northeastern Accelerators Personnel, Rev. Sci. Instrum. 57, 784 (1986).

"Organic Carbon-14 in the Amazon River System," J.I. Hedges, J.R. Hertl, P.D. Quay, P.M. Grootes, J. Richey, A.H. Devol, G.W. Farwell, P.H. Schmidt, and E. Salati, Science 231, 1129 (1986).

"Refractive Scattering and the Nuclear Rainbow in the Interaction of $^{12,13}C$ with $^{12}C$ at 20 MeV/N," H.G. Bohlen, X.S. Chen, J.G. Cramer, P. Frobrich, B. Gebauer, H. Lettau, A. Miczaika, W. von Oertzen, R. Ulrich, and T. Wilpert, Z. Phys. A 322, 241 (1985).

## Papers Submitted or in Press

"Giant Resonances in Excited Nuclei," K.A. Snover, Ann. Rev. Nucl. Part. Sci. (1986), to be published.

"Reply to 'Parity Violating Asymmetries in the Scattering of Transversely Polarized Protons'," E.G. Adelberger, P. Hoodbhoy, and B.A. Brown, Phys. Rev. C, to be published (1986).

"Fission Probes of Sub-Barrier Fusion Cross Section Enhancements and Spin Distribution Broadening," T. Murakami, C.-C. Sahm, R. Vandenbosch, D.D. Leach, A. Ray, and M.J. Murphy, Phys. Rev. C, accepted for publication.

"Nonequilibrium Population of Magnetic Substances and Excitation-Energy Division in the Decay of an Orbiting Complex," A. Ray, D.D. Leach, R. Vandenbosch, K.T. Lesko, and D. Shapira, submitted to Phys. Rev. Lett.

"Radiocarbon Dating with the University of Washington Accelerator Mass Spectrometry System," P.M. Grootes, M. Stuiver, G.W. Farwell, D.D. Leach, and F.H. Schmidt, Radiocarbon, in press.

"Rapid Response of Tree Cellulose Radiocarbon Content to Changes in Atmospheric $^{14}CO_2$ Concentration," G.W. Farwell, P.M. Grootes, D.D. Leach, F.H. Schmidt, and M. Stuiver, submitted to Tellus.

## Conference Presentations and Abstracts

"Energy Dependence of the Heavy Ion Total Reaction Cross Section of $^{12}C$ with $^{12}C$, $^{41}Ca$, $^{90}Zr$ and $^{208}Pb$," C.-C. Sahm, J.G. Cramer, A.J. Lazzarini, D.D. Leach, T. Murakami, D.R. Tieger, R.A. Loveman, W.G. Lynch, M.B. Tsang, and J. Van der Plicht, Bull. Am. Phys. Soc. 30, 1246 (1985).

"Inclusive Scattering of Pions from $^2$H, $^3$He, and $^4$He at 100 MeV," M.A. Khandaker, I. Halpern, D.D. Leach, T. Murakami, D.W. Storm, D.R. Tieger, J.F. Amann, W.J. Burger, K.G.R. Doss, and D.H. Dowell Bull. Am. Phys. Soc. 30, 1247 (1985).

"Excited-State Giant Dipole Resonances in $^{46}$Ti and $^{52}$Cr," G. Feldman, J.A. Behr, C.A. Gossett, J.H. Gundlach R. Loveman, J.L. Osborne, and K.A. Snover, Bull. Am. Phys. Soc. 30, 1256 (1985).

"High Energy Nonstatistical γ-rays from $^3$He- and $^4$He-Induced Reactions," J.A. Behr, K.A. Snover, C.A. Gossett, G. Feldman, and J.H. Gundlach, Bull. Am. Phys. Soc. 30, 1256 (1985).

"Statistical Decay of the Giant Dipole Resonances in Highly Excited Nuclei in the Mass Region A=70-90," J.H. Gundlach, J.A. Behr, G. Feldman, C.A. Gossett, and K.A. Snover, Bull. Am. Phys. Soc. 30, 1256 (1985).

"Astrophysical Implications of a Proposed High-Spin Isomer in $^{180}$Lu," S.E. Kellogg and E.B. Norman, Bull. Am. Phys. Soc. 30, 1274 (1985).

"Deformation of Heated Nuclei Observed in the Statistical Decay of the Giant Dipole Resonance," C.A. Gossett, (Invited Talk) Bull. Am. Phys. Soc. 30, 1278 (1985).

"Spin Distributions in Sub-Barrier Heavy Ion Fusion," T. Murakami, D.D. Leach, M.J. Murphy, A. Ray, C.C. Sahm, and R. Vandenbosch, Bull. Am. Phys. Soc. 30, 1279 (1985).

"Particle-γ and Particle-Particle Coincidence Probes of Orbiting in the $^{28}$Si+$^{12}$C," A. Ray, D. Leach, R. Vandenbosch, K.T. Lesko, and D. Shapira, Bull. Am. Phys. Soc. 30, 1280 (1985).

"$l$-Forbidden Beta Decay of $^{207}$Tl," M.M. Hindi, E.G. Adelberger, S.E. Kellogg, and T. Murakami, Bull. Am. Phys. Soc., submitted to Washington meeting, April 1986.

"The Calibration of Sub-Coulomb Heavy Ion Proton Transfer Reactions," K.J. Davis, T. Murakami, S. Gil, M. Khandaker, A. G. Lazzarini, D.D. Leach, R. A. Loveman, and J.L. Osborne Bull. Am. Phys. Soc., submitted to Washington meeting, April 1986.

"The University of Washington Super-Conducting Booster Linac," D.W. Storm, J.F. Amsbaugh, J.G. Cramer, H.E. Swanson, T.A. Trainor, R. Vandenbosch, W.G. Weitkamp, and D.I. Will, 1985 Particle Accelerator Conference, May 1985, Vancouver, Canada, IEEE Trans. on Nucl. Sci. 5, part II, 3262 (1985).

"Superconducting Resonators for the University of Washington Booster Linac," D.W. Storm, J.M. Brennan, and I. Ben-Zvi, 1985 Particle Accelerator Conference, May 1985, Vancouver, Canada, IEEE Trans. on Nucl. Sci. 5, part II, 3607 (1985).

"Rapid Response of Tree Ring Cellulose to Changing Atmospheric $^{14}CO_2$ Concentration," Abstract of paper presented at the 12th International Radiocarbon Conference, Norwegian Institute of Technology, Trondheim, Norway, June, 1985.

"Radiocarbon Dating with the University of Washington AMS System," G.W. Farwell, P.M. Grootes, F.H. Schmidt, and M. Stuiver, Abstract of paper presented at the 12th International Radiocarbon Conference, Norwegian Institute of Technology, Trondheim, Norway, June, 1985.

"Symmetries in Nuclei," E.G. Adelberger, Cretan International Meeting in Subatomic Physics, June 1985. Current Problems in Nuclear Physics, Demokritos, Aghia Paraskevi Greece. June 1985.

"The Nucleosynthesis of $^{180}Ta^m$ and the Mind of Man," S.E. Kellogg, 1985 Physics Summer Institute on Nuclear Astrophysics, University of Washington, Seattle, WA, July–Aug. 1985.

"Giant Resonances in Excited Nuclei," K.A. Snover 1985 Physics Summer Institute on Nuclear Astrophysics, University of Washington, Seattle, WA, July–Aug. 1985.

"Colliding-Beams Polarized Ion Source," T.A. Trainor, J.G. Douglas, D. Badt, C. Christiensen, A. Herron, D. Leach, J. Olson, J.L. Osborne, and V. Zeps, Proceedings of the Sixth International Symposium on Polarization Phenomena in Nuclear Physics, eds. M. Kondo, et al., 55, p. 1150 Osaka, Japan, August 1985.

"Polarization Transfer in $(\vec{d},\vec{p})$ Reactions," W.G. Weitkamp, published in the Proceedings of the Tsukuba International Workshop on Deuteron Involving Reactions and Polarization Phenomena, eds. Y. Aoki and K. Yagi, p. 13, Tsukuba, Japan, August 1985 (Invited paper).

"Radiocarbon Measurements with the University of Washington Accelerator Mass Spectrometry Facility," G.W. Farwell, Invited paper presented at the Symposium on Accelerator Mass Spectrometry, 19th National Meeting of the American Chemical Society on AMS, Sept. 85, Chicago, IL.

"The Nucleon-Nucleon Weak Interaction," E.G. Adelberger, National Bureau of Standards, Gaithersburg, MD, Nov. 1985.

"The Carbon-14 Activity of Organic Matter in Deep Sea Sediments: Preliminary Results," S.R. Emerson, C. Stump, P.M. Grootes, M Stuiver, G.W. Farwell, and F.H. Schmidt, Abstract of paper presented at the American Geophysical Union, New Orleans Meeting, January 1986.

"Anomalously Broad Spin Distributions in Sub-Barrier Fusion Reactions" C.-C. Sahm, T. Murakami, R. Vandenbosch, D.D. Leach, A. Ray, and M.J. Murphy, Contr. to Intern. Workshop on Gross Properties of Nuclei and Nuclear Excitations XIV, Hirschegg, Austria, Jan. 13–18, 1986.

"The Many Facets of Heavy Ion Fusion Reactions," R. Vandenbosch, Invited paper presented at the Symposium of The Many Facets of Heavy Ion Fusion Reactions, Argonne, IL, March 1986.

"Introduction," R. Vandenbosch, International Symposium on Nuclear Fission and Heavy-Ion-Induced Reactions, Rochester, NY, April, 1986.

"Weak and Electromagnetic Interactions in Nuclei," E.G. Adelberger, Symposium of Weak and Electromagnetic Interactions in Nuclei, Max-Planck Institut, Heidelberg, Germany, July, 1986.

"Nuclear Probes of Fundamental Symmetries," E.G. Adelberger International Symposium on Weak and Electromagnetic Interactions in Nuclei, Heidelberg, Germany, July, 1986.

"Giant Dipole Resonances in Excited Nuclei," K.A. Snover International Symposium on Weak and Electromagnetic Interactions in Nuclei, Heidelberg, Germany, July, 1986.

"Progress Report on an Experiment to Measure $\Delta I=0$ Parity Mixing in $^{14}N$," H.E. Swanson, V.J. Zeps, E.G. Adelberger, C.A. Gossett, J. Stromecki, W. Haeberli, P. Quin. International Symposium on Weak and Electromagnetic Interactions in Nuclei, Heidelberg, Germany, July, 1986.

Other Publications by Members of the Laboratory and Other Laboratory Research:

"Alpha Transfer Reaction $^{16}O(^{12}C,^{8}Be_{g.s.})^{20}Ne$: Key Process in the $^{12}C(^{16}O,\alpha)$ Reaction," T. Murakami, E. Ungricht, W. Lui, Y. Mihara, E. Takada, and R.E. Tribble, Phys. Rev. C $\underline{32}$, 1558 (1985).

"Search for a Direct Large-Cluster-Transfer Process in the $^{12,13}C(^{20}Ne,\alpha)$ Reaction," T. Murakami, N. Takahashi, Y.-W. Lui, E. Takada, D.M. Tanner, R.E. Tribble, E. Ungricht, and K. Nagatani, Phys. Rev. C $\underline{32}$, 2161 (1985).

Linear Momentum and Angular Momentum Transfer in the Reaction of $^{16}O$ with $^{154}Sm$," M.N. Namboodiri, R.K. Choudhury, L. Adler, J.D. Bronson, D. Fabris, U. Garg, P.L. Gonthier, K. Hagel, D.R. Haenni, Y.W. Lui, Z. Majka, G. Mouchaty, T. Murakami, J.B. Natowitz, G. Nebbia, R.P. Schmitt, S. Simon, J.P. Sullivan, and D.H. Youngblood, submitted to Phys. Rev. C.

"Fusion Probability of Symmetric Heavy, Nuclear Systems Determined from Evaporation Residue Cross Sections," C.-C. Sahm, H.-G. Clerc, K.-H. Schmidt, W. Reisdorf, P. Armbruster, F.P. Hessberger, J.G. Keller, G. Münzenberg, and D. Vermeulen, Nucl. Phys. A $\underline{441}$, 316 (1985).

"Fusability in $^{86}Kr$-induced Reactions near and below the Fusion Barrier," W. Reisdorf, F.P. Hessberger, K.D. Hildenbrand, S. Hofmann, G. Münzenberg, K.-H. Schmidt, W.F.W. Schneider, K. Suemmerer, G. Wirth, J.V. Kratz, K. Schlitt, and C.-C. Sahm, Nucl. Phys. A $\underline{444}$, 154(1985).

"The New Isotopes $^{256}$105, $^{257}$105, $^{254}$Lr and $^{253}$Lr," F.P Hessberger, G. Münzenberg, S. Hofmann, Y.K. Agarwal, K. Poppensieker, W. Reisdorf, K.-H. Schmidt, J.R.H. Schneider, W.F.W. Schneider, H.J. Schött, P. Armbruster, B. Thuma, C.-C. Sahm, and D. Vermeulen, Z. Phys. A $\underline{322}$, 557 (1985).

"Gamma-Spectroscopic Investigations in the Radiative Fusion Reaction $^{90}$Zr + $^{90}$Zr," K.-H. Schmidt, R.S. Simon, J.G. Keller, F.P. Hessberger, G. Münzenberg, B. Quint, H.-G Clerc, W. Schwab, U. Gollerthan, and C.-C. Sahm, submitted to Phys. Lett. B.

"Cold Fusion in Symmetric $^{90}$Zr Induced Reactions," J.G. Keller, K.-H. Schmidt, F.P. Hessberger, G. Münzenberg, W. Reisdorf, H.-G Clerc, and C.-C. Sahm, submitted to Nucl. Phys. A.

FRONT ROW: CONNOLLY, ROSENZWEIG, WILL, BEHR, KICINSKA, KHANDAKER, FERNANDEZ, FULTON, VANDENBOSCH, MALKASIAN, RAMIREZ, DOUGLAS, SCHMIDT, READDY, NEWELL, SCOTT

MIDDLE ROW: KELLOGG, EROMIE, LIN, GUNDLACH, SNOVER, TOMASKO, PASCHKE, DAVIS, J., CORCORAN, STOWELL, SIMA, HINN, FAUSKA, WONG, DAVIS, K., FARNELL, SIMONS, CRAMER, WETTKAMP, GROOTES, BALSLEY, WOOTRESS, FELDMAN

BACK ROW: BADT, BLACK, IRWIN, MEADOWS, HOWE, HOLM, VAN WECHEL, MORRIS, GLATZEL, FLOYD, HODGKINS, MCMURRY, HALPERN, LAKRDIX, LINDER, LU, SEYMOUR